

## MSc BioMedical Engineering

# Heart-on-chip: functional lipoprotein lipase (LPL) expression in co-cultures of cardiomyocytes and endothelial cells

## Master thesis

Student name: **Lisanne L. Blauw**

Student number: 4477340

Delft University of Technology

Faculty: Mechanical, Maritime, and Materials Engineering (3mE)  
Department: BioMechanical Engineering  
MSc Specialization: Biomaterials & Tissue Biomechanics  
MSc thesis advisor: Dr. ir. Iulian Apachitei and Prof. dr. Amir Zadpoor  
External supervisors: Dr. Marcelo Ribeiro and Prof. dr. Robert Passier  
Date: September 13, 2019

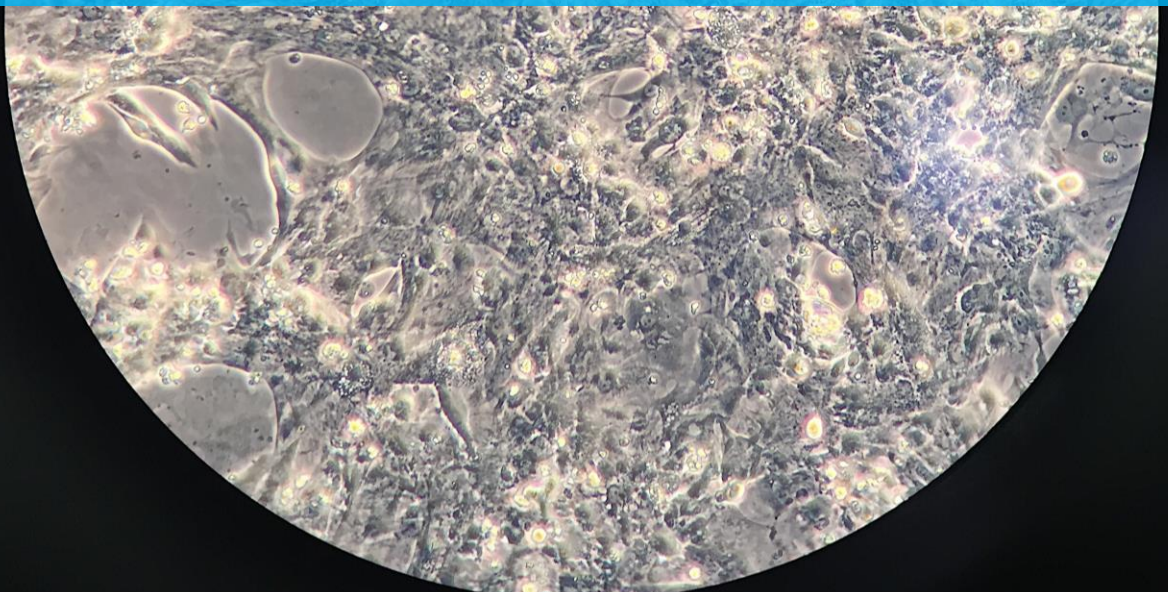


# Table of contents

<b>Abstract</b> .....	<b>3</b>
<b>1. Introduction</b> .....	<b>4</b>
1.1 Clinical relevance .....	4
1.2 Lipoprotein lipase .....	5
1.3 Energy metabolism of the heart.....	6
1.4 Pluripotent stem cells .....	7
1.5 Metabolic maturation of cardiomyocytes <i>in vitro</i> .....	7
1.6 Study aims .....	8
<b>2. Materials &amp; methods</b> .....	<b>9</b>
2.1 Experiment planning.....	9
2.2 Cell culturing .....	14
2.3 Fatty acid uptake by the cells .....	15
2.4 LPL activity in the medium.....	16
2.5 RNA purification and quantitative real-time polymerase chain reaction (qRT-PCR) ...	16
2.6 Western blotting .....	18
2.7 Statistics .....	19
2.8 Chip design .....	19
<b>3. Results</b> .....	<b>22</b>
3.1 Pilot experiment: LPL activity in the medium .....	22
3.2 Fatty acid uptake and LPL activity in different cell cultures .....	22
3.3 Effects of particle incubation time on fatty acid uptake.....	25
3.4 Dependency of fatty acid uptake on ApoC2.....	26
3.5 Presence of LPL protein in the medium .....	27
3.6 Chip design.....	28
<b>4. Discussion</b> .....	<b>31</b>
<b>5. Conclusion</b> .....	<b>36</b>
<b>6. Future considerations</b> .....	<b>37</b>
<b>Acknowledgements</b> .....	<b>38</b>
<b>Appendix</b> .....	<b>43</b>
Expanded methods .....	43
Supplementary tables .....	48
Supplementary figures .....	50
<b>Glossary</b> .....	<b>54</b>

# Abstract

**Introduction** | Cardiovascular diseases (CVD) are the number one cause of death worldwide. Individuals with a high risk of developing CVD are nowadays mainly treated with cholesterol lowering drugs. Although disease risk can be lowered by a maximum of 40% in this way, a significant untreatable residual risk is left. Therefore, there is a big quest to find novel medicines. The enzyme lipoprotein lipase (LPL) is a key player in lipid metabolism and has recently gained a lot of attention as novel druggable target for CVD risk reduction. Although identification of LPL-activating small molecules is eagerly awaited, screening of compound libraries is nowadays impossible, as it is extremely challenging to study LPL activity in an *in vitro* setting due to its complex mode of action, which requires direct crosstalk between endothelial cells and metabolically active tissue. Therefore, the overall objective is to use organ-on-chip technology to develop a predictable *in vitro* model for functional LPL activity. Such a model is a giant leap in CVD modelling, and will open the door for discovery and development of new therapeutics for this deadly disease.

**Study aims** | My master thesis project was the start of the overall project, and therefore mainly focused on general characterization of LPL activity in different cell types, with the aim to 1) determine the difference in fatty acid uptake and LPL activity in the medium between cardiomyocyte monocultures, cardiomyocyte endothelial cell co-cultures and endothelial cell monocultures *in vitro*; 2) define optimal culturing conditions for high LPL activity; and 3) design a heart-on-chip model to co-culture 3D cardiac tissue and endothelial cells such that they are in direct contact with each other. The hypothesis is that co-culturing increases functional LPL activity.

**Methods** | Fatty acid uptake and LPL activity was compared between human pluripotent stem cell (hPSC)-derived cardiomyocyte monocultures, cardiomyocyte-endothelial cell co-cultures and endothelial cell monocultures, using tri<sup>3</sup>H]oleate and [<sup>14</sup>C]cholesteryl oleate double radioactively labeled triglyceride-rich lipoprotein (TRL)-mimicking particles. The heart-on-chip was designed with Solidworks software.

**Results** | LPL activity in the medium, measured as triglyceride-derived fatty acid release, was highest in co-cultures. Fatty acid uptake by the cells also seemed to be higher in co-cultures than cardiomyocyte monocultures, although differences were not statistically significant. Endothelial cells consistently showed lowest fatty acid uptake. Importantly, incubation of TRL-mimicking particles with ApoC2, which is an essential co-factor of LPL enzymatic activity, drastically increased fatty acid uptake by cardiomyocytes and co-cultures.

**Conclusions** | The results strongly indicate that co-culturing cardiomyocytes with endothelial cells, compared to monocultures, increases fatty acid uptake by the cells and triglyceride-derived free fatty acid release in the cell culture medium, both being indicators of increased functional LPL activity. For highest LPL activity, experimental conditions should include incubation of TRL-mimicking particles with at least 0.25 µL/well ApoC2 and a particle incubation time of at least 4 hours. The future goal is to repeat the current experiments in a 3D setting using the designed heart-on-chip model.

# 1. Introduction

## 1.1 Clinical relevance

Cardiovascular diseases are the number one cause of death worldwide, claiming 17.9 million deaths per year.<sup>1</sup> Most deaths are due to ischemic heart disease,<sup>2</sup> which is mostly caused by narrowing of the coronary arteries as a consequence of atherosclerosis that is characterized by accumulation of cholesterol in the arterial wall. To prevent atherosclerosis formation, drugs have been developed to lower low-density lipoprotein (LDL, *see Glossary for more explanation on abbreviations*) particles, which are the main carriers of cholesterol (C) in the circulation.<sup>3</sup> The most prescribed drugs are statins,<sup>4</sup> which can lower the risk of cardiovascular events up to 40%.<sup>4</sup> More recently, proprotein convertase subtilisin/kexin type 9 (PCSK9) inhibitors were developed, which decrease the disease risk by an additional 15% on top of statin therapy.<sup>5</sup> However, disease risk is still far from reduced to zero. Moreover, the relatively small risk reduction of the new PCSK9 inhibitors combined with their high price, costing over \$12,000 a year per patient,<sup>6</sup> restricts their prescription. This further stresses the urgent need for novel therapies to reduce cardiovascular disease burden, especially in light of future trends towards ageing populations and more unhealthy lifestyles.

Recently, elevated triglyceride concentrations were identified as important additional risk factor for cardiovascular disease.<sup>7,8</sup> Specifically, triglyceride-rich lipoprotein (TRL) remnants enriched in cholesterol, which are derived from chylomicrons and very low-density lipoprotein (VLDL) particles, seem to be the culprit responsible for atherosclerosis formation.<sup>9</sup> The so called 'remnant cholesterol' in these particles is associated with a 2.8-fold increased risk of ischemic heart disease.<sup>10</sup> **Figure 1** shows the general structure of a lipoprotein. Obviously, pharmaceutical industry is now looking for strategies to reduce circulating TRLs. Since lipoprotein lipase (LPL) is a key player in TRL metabolism, this enzyme has recently arisen as a novel highly promising target for cardiovascular disease risk reduction.

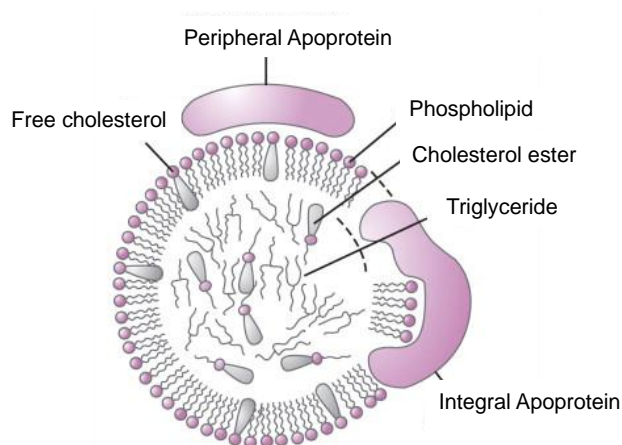


**Figure 1 – Structure of a lipoprotein.** The shell of the lipoprotein is built out of phospholipids, free cholesterol and various apolipoproteins. The core consists of cholesterol esters and triglycerides. Figure derived from <sup>11</sup>.

## 1.2 Lipoprotein lipase

LPL plays a key role in energy metabolism by supplying metabolically active tissues with fuel in the form of fatty acids. Triglycerides derived from the core of TRLs are hydrolyzed by LPL into free fatty acids, which are subsequently taken up by energy-demanding tissues, while generated TRL remnants are avidly taken up by the liver. As outlined in **Figure 2**, LPL is synthesized by parenchymal cells of metabolically active tissues (e.g. cardiomyocytes, which are the contractile muscle cells of the heart), but to be functional it needs to anchor to the luminal surface of endothelial cells via a binding protein (i.e. glycosylphosphatidylinositol anchored high density lipoprotein binding protein 1, GPIHBP1). LPL on endothelial cells liberates free fatty acids from TRL particles, which are then transported to the underlying tissue via cell surface receptors on both endothelial cells and parenchymal cells (mainly via cluster of differentiation 36, CD36).<sup>12-17</sup> In fact, if LPL does not become attached to endothelial cells, it is converted into inactive monomers and loses its enzymatic activity, such that fatty acids cannot be released from TRLs (**Figure 2.Left**).<sup>18-20</sup> LPL is most abundantly expressed in energy-demanding tissues, including the heart (cardiomyocytes) and fat tissue (adipocytes).<sup>16</sup>

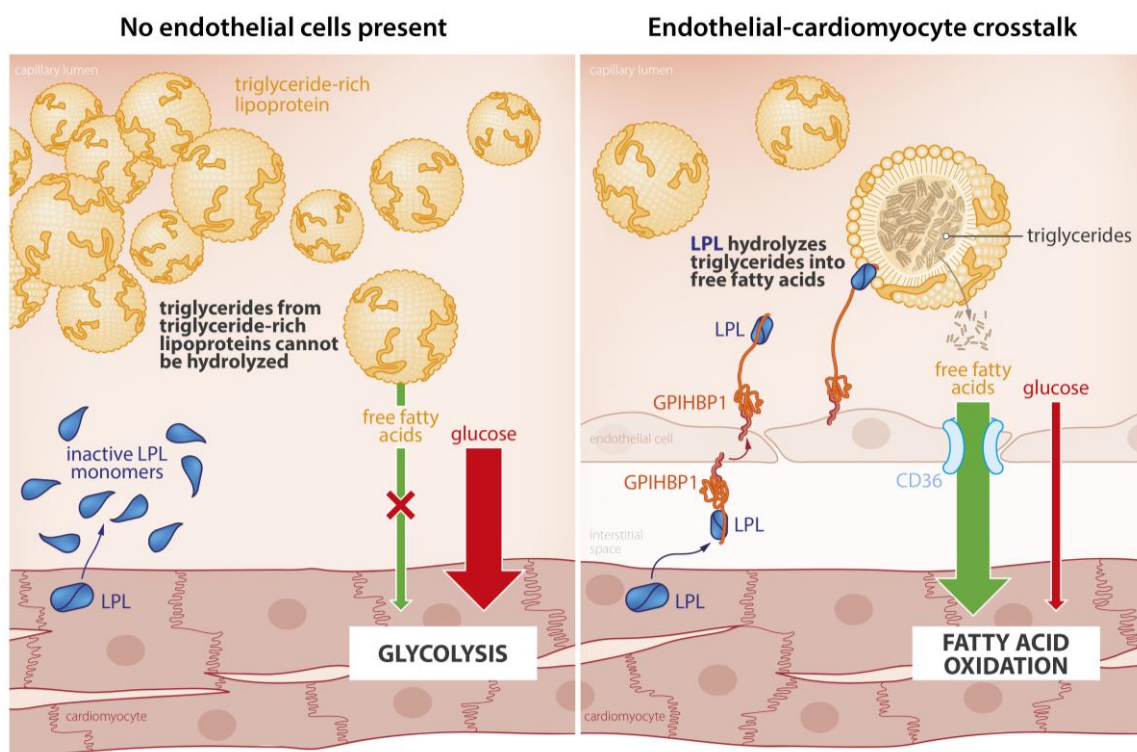


**Figure 2 – Hypothesis: a crosstalk between endothelial cells and cardiomyocytes is essential for LPL activity.** **Left:** In the absence of endothelial cells, LPL is secreted by cardiomyocytes and directly falls apart into inactive monomers. Thus, triglycerides from triglyceride-rich lipoproteins (TRLs) cannot be hydrolyzed and the cardiomyocytes are dependent on glucose for their energy supply. In an *in vivo* setting, TRLs would then pile up in the blood stream. **Right:** When endothelial cells are present, they express GPIHBP1 that binds LPL in the interstitial space for transport to the luminal side of the endothelial cells, where LPL binds circulating TRLs in order to hydrolyze triglycerides into free fatty acids. The liberated free fatty acids can then be transported to the cardiomyocytes to be used as energy source. Figure designed in collaboration with Manon Zuurmond (graphical designer, Leiden University Medical Center).

LPL is modulated by a wide range of circulating proteins that either inhibit or enhance its enzymatic activity. The LPL inhibitors angiopoietin-like 3 (Angptl3) and apolipoprotein (Apo) C3 have been pointed out by genetic studies as targets for cardiovascular disease risk reduction.<sup>7,8,21,22</sup> With LPL being identified as the new top target for cardiovascular risk reduction, pharmaceutical companies are currently massively investing in drug discovery programs for LPL enhancing therapies, evidenced by the ongoing clinical trials with Angptl3 and ApoC3 inhibitors. Moreover, *in vivo* studies have revealed other circulating proteins to either stimulate (e.g. ApoC2, ApoA5) or inhibit (e.g. ApoC1, ApoC3) LPL activity,<sup>16,23-26</sup> which are all possible promising druggable targets for TRL remnant lowering.

Besides these endogenous proteins, identification of LPL-activating small molecules is eagerly awaited. However, screening large compound libraries for effectiveness in human cells is nowadays impossible, as it is extremely challenging to study LPL activity in an *in vitro* setting due to its complicated mode of action. As outlined above, expression of enzymatically active LPL requires interaction between endothelial cells with the underlying tissue (such as cardiomyocytes), and a 3D orientation of the blood vessel lumen and interstitial space, which cannot be mimicked by a simple monolayer of cells in a culture dish. This is probably the reason that *in vitro* single cell cultures mainly use glucose, while *in vivo* metabolically active cells also use fatty acids for their energy supply (**Figure 1**). Therefore, a human *in vitro* model of 3D interaction between endothelial and parenchymal cells is eagerly needed to study the modulation of LPL. In this project, we focus specifically on the heart.

### 1.3 Energy metabolism of the heart

All human cells rely on carbohydrate and fatty acid oxidation for their energy supply. The ratio between these two forms of substrate oxidation is dependent on the tissue type. The heart possesses a great metabolic flexibility and is able to change its substrate preference based on a variety of external factors, including hormone concentrations, coronary flow, nutritional state and tissue pathophysiology.<sup>27,28</sup> The healthy human adult heart is fueled for 60-90% by fatty acids,<sup>28,29</sup> whereas the minority of energy (10-40%) comes from pyruvate that is derived from either glucose or lactate oxidation.<sup>28</sup> Both pathways produce energy in the form of adenosine triphosphate (ATP). ATP is mainly used for shortening of cardiomyocytes and functioning of ion pumps, which are critical to maintain the contractile function of the heart.<sup>28</sup> Complete turnover of the ATP content takes only 10 seconds under normal conditions, putting a high pressure on energy generation.<sup>28</sup> Energy metabolism of the heart is therefore tightly regulated, whereby the rate of oxidative phosphorylation is directly adapted to the hydrolysis of ATP, such that the total ATP content stays constant.<sup>28,30</sup>

The two main metabolic pathways for energy production in the heart are glycolysis and beta oxidation.<sup>31,32</sup> During glycolysis glucose is converted to pyruvate, whereby two ATP molecules are formed for every glucose molecule. This process does not require oxygen (anaerobic). The formed pyruvate can then be used to form lactate (anaerobic pathway) or be shuttled to the

mitochondria to form acetyl coenzyme A (acetyl-CoA), which is the fuel for oxidative phosphorylation. The other pathway to generate acetyl-CoA is beta-oxidation, whereby acetyl-CoA is generated from fatty acids. In the heart, the majority of acetyl-CoA used for oxidative phosphorylation is derived from fatty acids.<sup>28</sup> During oxidative phosphorylation acetyl-CoA is oxidized in a chain reaction that leads to the formation of hydrogen carriers that enter the electron transport chain, where they create an electrochemical proton gradient that facilitates the production of ATP.<sup>31</sup>

If sufficient oxygen is present (aerobic conditions), ATP production in the heart is for 95% derived from oxidative phosphorylation, as this is by far the most efficient pathway to produce ATP.<sup>31</sup> To compare, oxidative phosphorylation generates 36 ATP per glucose molecule, whereas glycolysis produces only 2 ATP per glucose molecule. Fatty acids yield an even higher ATP production per carbon atom during oxidative phosphorylation, however, fatty acid oxidation requires a higher amount of oxygen, as compared to glucose.<sup>31</sup>

## 1.4 Pluripotent stem cells

To mimic the *in vivo* human situation as close as possible, we used healthy human cells for this project. Both cardiomyocytes and endothelial cells were derived from human pluripotent stem cells (hPSC). These hPSCs can be generated from either human embryonic cells or human somatic cells (human induced pluripotent stem cells, hiPSC) and have the capacity to be expanded *in vitro* and differentiated to any cell type of the human body.

There has been a lot of research performed on defining the best protocols to differentiate these stem cells into adult-like cells. Although standardized differentiation protocols for hPSC into tissue-specific cell types are widely available, it remains challenging to resemble adult *in vivo* cells as close as possible. Especially in the cardiac field of hPSC the so called 'immaturity' of hPSC-derived heart cells is an important unsolved problem.

As immature cells do not reliably mimic the real human heart, optimal use of healthy as well as disease cell lines as a solid platform for disease modelling and drug testing has been hampered. Specifically, disease modelling of metabolic diseases and diseases that are caused by disturbed energy metabolism cannot be reliably mimicked *in vitro*. Therefore, the quest for increasing cell maturity of cardiomyocytes is currently a main focus of the field.

## 1.5 Metabolic maturation of cardiomyocytes *in vitro*

Besides creating an *in vitro* model with functional LPL activity that can be used for drug screening, we also aim to more closely mimic the behavior of *in vivo* cardiomyocytes by increasing the metabolic maturation of hPSC-derived cardiomyocytes. One of the main features of incomplete hPSC-cardiomyocyte maturation is their immature metabolism compared with *in vivo* adult cardiomyocytes.<sup>33,34</sup> The human heart is fueled for 60-70% by

triglyceride-derived fatty acids,<sup>29</sup> while hPSC-cardiomyocytes cultured *in vitro* almost only use glucose as their energy source.

The metabolism of hPSC-cardiomyocytes is comparable to that of the fetal human heart, which relies mainly on glycolysis for its energy supply due to the low oxygen and fatty acid concentration in the uterus environment.<sup>31,35</sup> When cardiomyocytes become terminally differentiated after birth, so called mature cardiomyocytes, their metabolism switches from glycolysis to fatty acid-based oxidative phosphorylation.<sup>31,35</sup> This metabolic switch is crucial to fulfill the high demand of ATP necessary for increased workload of the heart, which cannot be provided by glycolysis alone.<sup>31</sup> The switch is induced by the increased availability of oxygen and fatty acids after birth,<sup>31,36</sup> but the exact underlying mechanism that leads to alterations in the transcriptional control of the pathways is not well understood. Until now, scientists have not succeeded to induce a similar metabolic switch in hPSC-cardiomyocytes, which is a key limiting factor for their maturation *in vitro*. The unsolved problem here is that *in vitro* hPSC-cardiomyocytes are not able to take up free fatty acids for their energy supply. A more in-depth review on this topic is described in my Literature Study "*The importance of energy metabolism for human induced pluripotent stem cell-derived cardiomyocyte maturation*".

## 1.6 Study aims

The overall aim of this project is to develop a 3D heart-on-chip model that mimics human *in vivo*-like endothelial-cardiomyocyte interaction, in order to create a model for functional LPL activity *in vitro*. Such a model is a giant leap in cardiovascular disease modelling, and will open the door for discovery and development of new therapeutics for this deadly disease.

My master thesis project was the start of the overall project, and therefore mainly focused on general characterization of LPL activity in the different cell types. The specific aims were:

1. Determine the difference in fatty acid uptake and LPL activity in the medium between hPSC cardiomyocyte monocultures, cardiomyocyte endothelial cell co-cultures and endothelial cell monocultures *in vitro* (2D culture plates)
2. Define optimal culturing conditions for high LPL activity *in vitro* (2D culture plates)
3. Design a heart-on-chip model to co-culture 3D cardiac tissue and endothelial cells such that they are in direct contact with each other

The hypothesis is that co-culturing increases functional LPL activity, according to the mechanism explained in **Figure 2**.

## 2. Materials & methods

### 2.1 Experiment planning

In all experiments three groups were compared: 1) cardiomyocyte monocultures, 2) cardiomyocyte-endothelial cell co-cultures and 3) endothelial cell monocultures. From now on, in short described as cardiomyocytes, co-cultures and endothelial cells. In total, five different research questions were answered, which are described in below, to fulfill the study aims.

- **Pilot experiment - LPL activity in the medium**

*Is there a difference in LPL activity in the medium of cardiomyocyte monocultures versus cardiomyocytes-endothelial cell co-cultures?*

LPL activity in the medium was compared between the two groups. A positive result from this experiment was an important indicator to proceed with the project.

- **Fatty acid uptake and LPL activity in different cell cultures**

*Is there a difference in fatty acid uptake between the three different cell groups?*

Fatty acid uptake by the cells and LPL activity in the medium (repetition pilot experiment) was compared between the three cell groups. Cells were collected for RNA extraction. For fatty acid uptake analyses, two out of four wells per cell type were treated with ApoC2, which is a co-factor for LPL enzymatic activity. **Figure 3** and **Figure 4** show the experiment planning and design, respectively.

**Co-culture experiment 2 | Jan/Feb 2019**  
 For LPL assay and particle experiment  
 Performed on 12 wells plate: total 24 wells

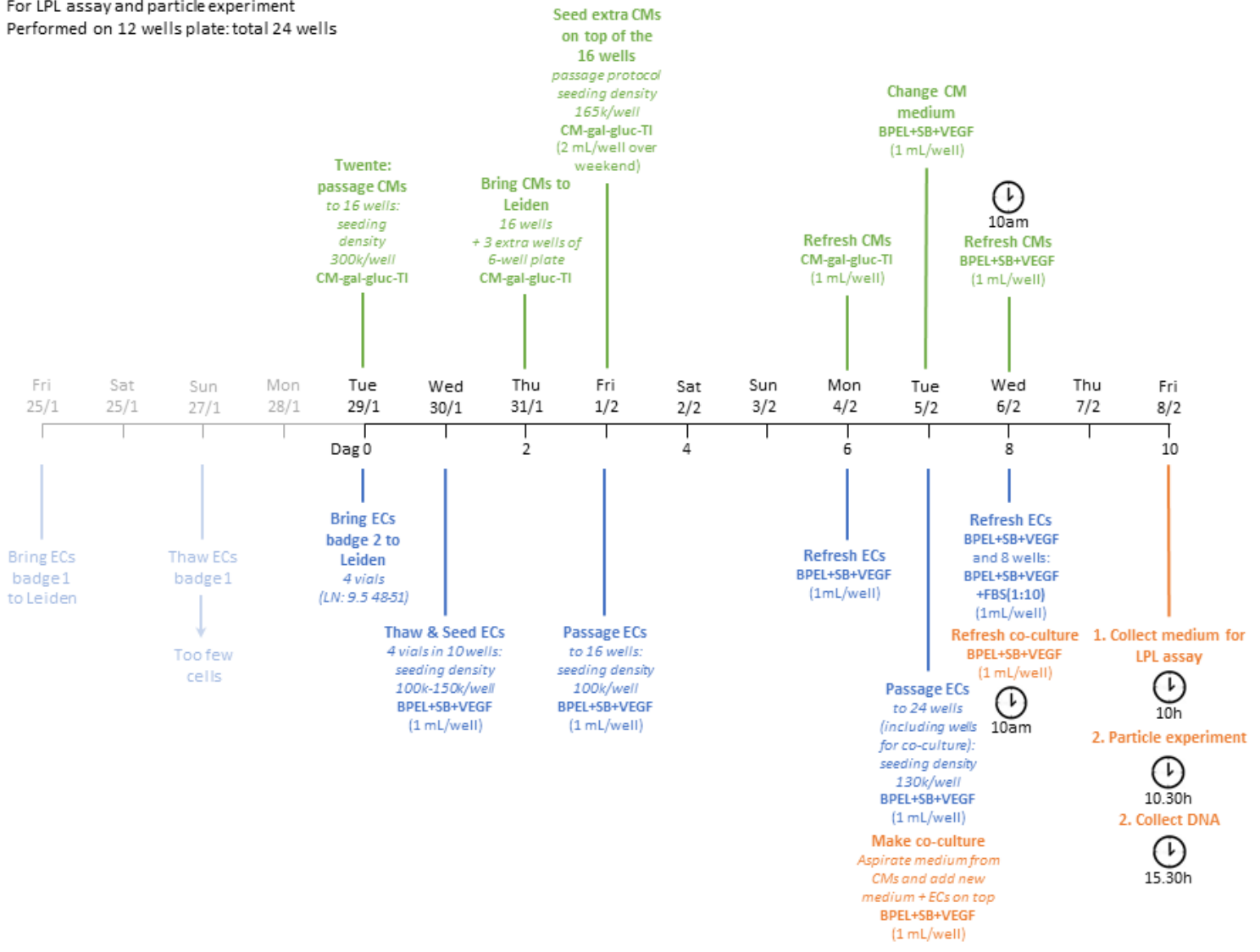


**Figure 3.** Experiment planning “Fatty acid uptake and LPL activity in different cell cultures”. BPEL+SB+VEGF, medium for endothelial cells and co-cultures (see Methods for explanation), CM, cardiomyocytes; CM-gal-gluc-TI, medium for cardiomyocytes (see Methods for explanation); EC, endothelial cells.

Co-culture experiment 2 | Jan/Feb 2019  
Plate layout 5 Feb 2019

Sample storage

LPL assay: 34\* medium samples @ -80, 16 DNA samples @ -20

\* Eppendorf 17 is clean sample of BPEL+VEGF+SB and Eppendorf 18 is BPEL+VEGF+SB+FBS

Particle experiment: 16 plasma samples @ -20

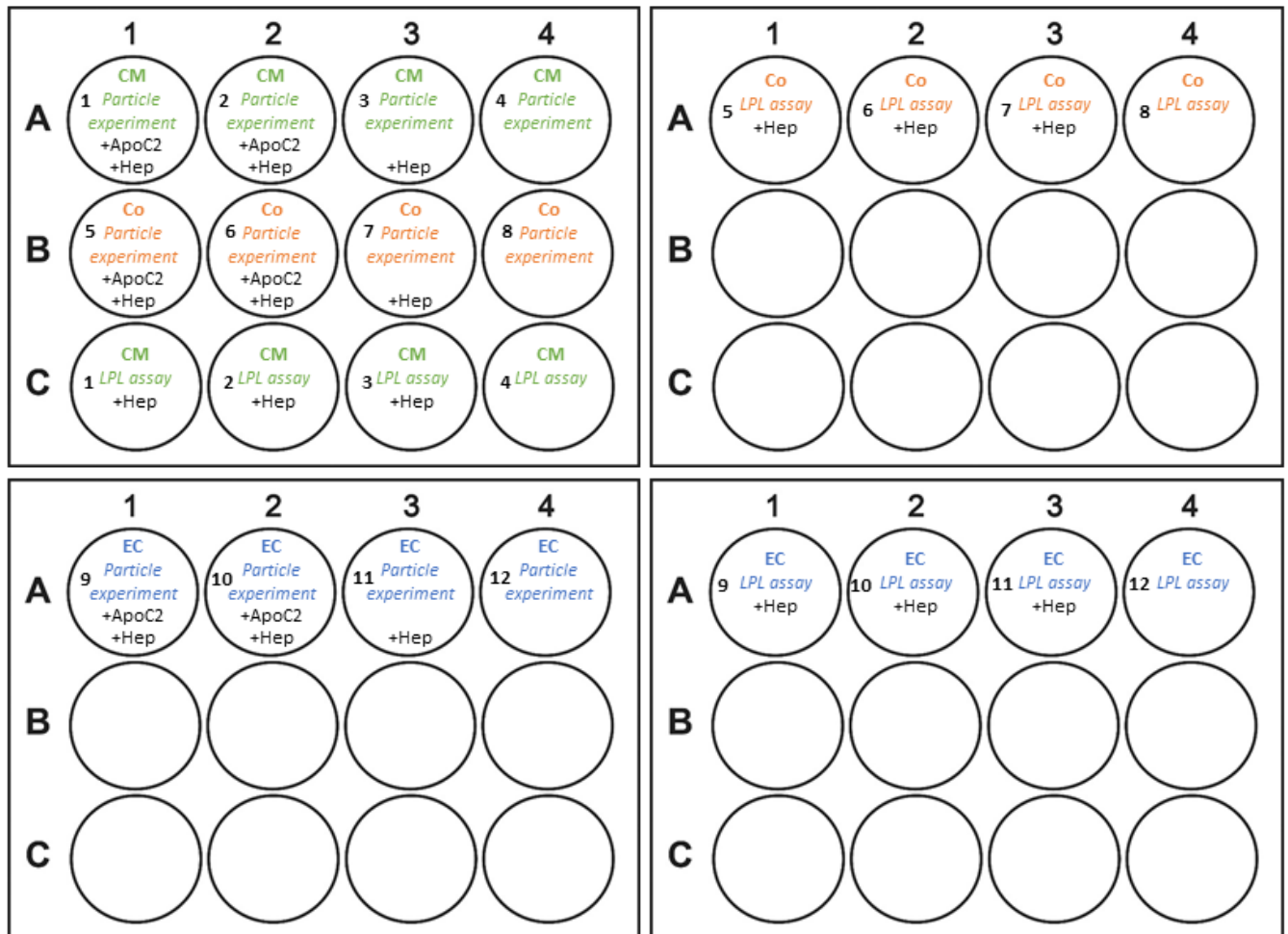


**Figure 4.** Cell culture well lay-out “Fatty acid uptake and LPL activity in different cell cultures”, showing the cell cultures per well. ApoC2, apolipoprotein C2; CM, cardiomyocyte; Co, co-cultures; Diff, day of start differentiation; EC, endothelial cell; Hep, heparin.

- **Effects of particle incubation time on fatty acid uptake**

*At what particle incubation time is fatty acid uptake by the cells highest?*

Fatty acid uptake by the cells was assessed after different incubation times of TRL-mimicking particles in the culture medium, i.e. 15 minutes, 30 minutes, 1 hour, 2 hours and 4 hours. For all groups ApoC2 was added. **Figure 5** shows the experiment design. The detailed experiment planning can be found in **Supplementary figure 1**.

Co-culture experiment 3 | April 2019  
 Plate layout 26 April 2019

Sample storage  
 Particle experiment: 60 plasma samples @ -20

NOTE: All well are +ApoC2

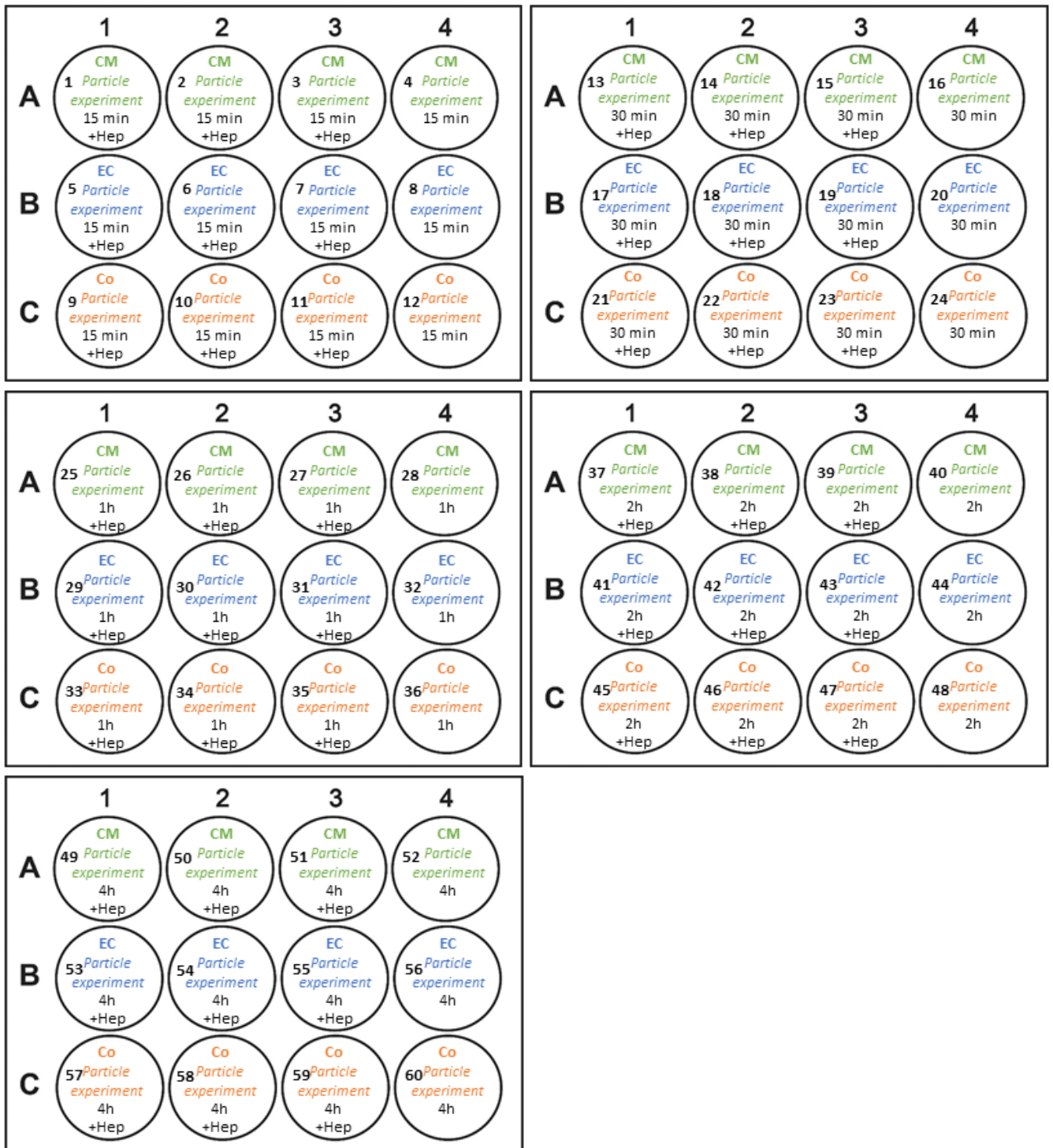
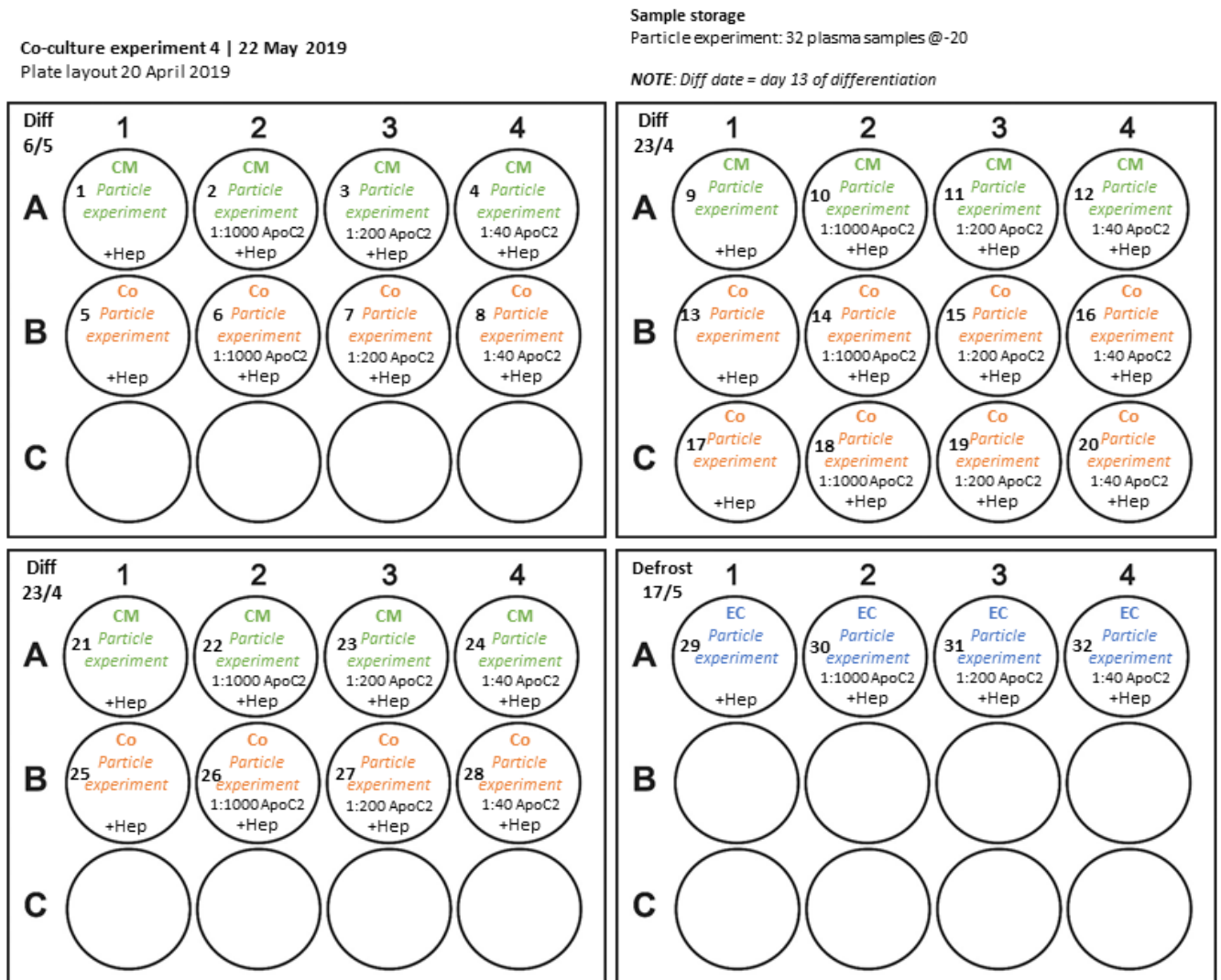


Figure 5. Cell culture well lay-out “Effects of particle incubation time on fatty acid uptake”, showing the cell cultures per well. CM, cardiomyocyte; Co, co-cultures; EC, endothelial cell; Hep, heparin.

▪ **Dependency of fatty acid uptake on ApoC2**

*Is fatty acid uptake dependent on ApoC2 concentration, as ApoC2 is an essential co-factor of LPL?*

Fatty acid uptake by the cells was assessed for different concentrations of ApoC2, which was incubated with the TRL-mimicking particles before the particles were added to the culture medium. **Figure 6** shows the experiment design. The detailed experiment planning can be found in **Supplementary figure 2**.



**Figure 6.** Cell culture well lay-out “Dependency of fatty acid uptake on ApoC2”, showing the cell cultures per well. ApoC2, apolipoprotein C2; CM, cardiomyocyte; Co, co-cultures; Diff, day of start differentiation; EC, endothelial cell; Hep, heparin.

- **Presence of LPL protein in the medium**

*Is LPL protein excreted by the cells and present in the medium?*

LPL protein in the medium was determined by Western blotting. **Figure 7** shows the experiment design. The detailed experiment planning can be found in **Supplementary figure 3**.

Co-culture experiment 5 | June 2019  
Plate layout 3 June 2019

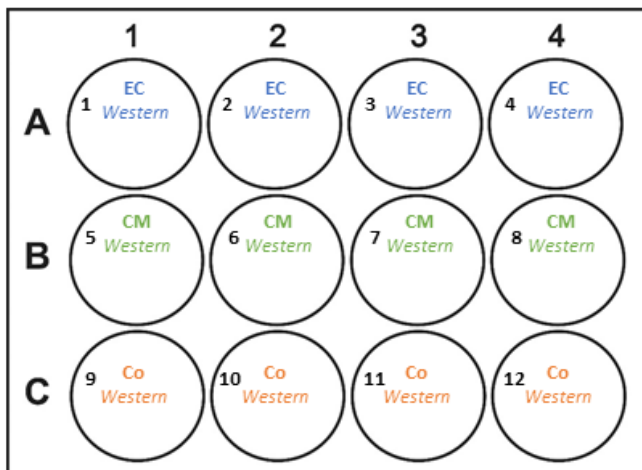


**Figure 7.** Cell culture well lay-out “Presence of LPL protein in the medium”, showing the cell cultures per well. CM, cardiomyocyte; Co, co-cultures; EC, endothelial cell.

This project is a collaborative project between the Department of Applied Stem Cell Technologies, University of Twente (UT) and the Department of Internal Medicine, Division of Endocrinology, Leiden University Medical Center (LUMC). Apart from the pilot experiments, all experiments were performed in the LUMC, as the fatty acid uptake experiments require a laboratory suited for the use of radioactive material, which is available at LUMC. All radioactive experiments were performed under supervision of a qualified laboratory technician. Cardiomyocytes and endothelial cells were cultured in the University of Twente and transported to the LUMC, either frozen on dry ice (endothelial cells) or alive at room temperature (cardiomyocytes).

## 2.2 Cell culturing

Cardiomyocytes were differentiated from an embryonic hPSC line by a laboratory technician (Department of Applied Stem Cell Technologies, UT) according to a previously published protocol.<sup>37</sup> From day 13 up to day 20 of differentiation, cardiomyocytes were dissociated and subsequently seeded for experiments. Cardiomyocytes were dissociated with TrypLE select (Gibco) for 10 minutes at 37°C and plated in 1 mL of medium at a density of 500,000 to 600,000 cells/well on 12 well culture plates, which were pre-coated with Matrigel (Corning, USA) to promote cell adhesion and cardiogenesis.<sup>38,39</sup> Cells were counted with a hemocytometer. Culture medium was non-enriched glucose cardiomyocytes medium that was supplemented with triiodothyronine (T3), hydrochloric acid (HCl), insulin like-growth factor (IGF) and glucose,

i.e. cardiomyocyte maturation medium. Medium was refreshed every 3 days. See **Appendix Expanded Methods A.1** for the cell culturing protocol and medium formulation.

Endothelial cells were differentiated from a hiPSC by a laboratory technician (Department of Applied Stem Cell Technologies, UT) and stored in liquid nitrogen, according to an in-house protocol developed by V. Schwach. For experiments endothelial cells were defrosted and plated in 1 mL medium at a density of 100,000 cells/well on 12 well culture plates, which were pre-coated with a fibronectin solution to promote cell adhesion and growth.<sup>40</sup> Cells were counted with a hemocytometer. Culture medium was bovine serum albumin (BSA) polyvinylalcohol essentials lipids (BPEL) medium that was supplemented with vascular endothelial growth factor (VEGF) and transforming growth factor- $\beta$  pathway small-molecule inhibitor SB431542 (SB), which support the expansion of endothelial cells.<sup>41</sup> Cells were passaged at 80% to 90% confluency until the preferred amount of cells for the experiment was reached, with a maximum of three passages. For passaging, cells were dissociated with TrypLE select (Gibco) for 3 minutes at 37°C and seeded in 1 mL BPEL medium supplemented with VEGF and SB at a density of 100,000 cells/well on 12 well culture plates, which were pre-coated with a fibronectin solution. Medium was refreshed every 3 days. See **Appendix Expanded Methods A.2** for the cell culturing and passaging protocols.

Co-cultures were made by seeding endothelial cells on top of the cardiomyocyte cultures. For that, cardiomyocyte maturation medium was removed from the cardiomyocyte cultures and endothelial cells were seeded on top in 1 mL BPEL medium supplemented with VEGF and SB at a density of 100,000 cells/well. At the moment the co-cultures were made, cardiomyocyte monocultures were also changed from cardiomyocyte maturation medium to 1 mL BPEL supplemented with VEGF and SB, to keep culture conditioned the same between groups.

All procedures were according to ethical guidelines, and informed consent for the use of these cells was obtained.

### 2.3 Fatty acid uptake by the cells

A labelled particle uptake assay was performed to reveal the uptake ratio of <sup>3</sup>H versus <sup>14</sup>C by the cells, where <sup>3</sup>H is a measure for fatty acids uptake and <sup>14</sup>C a measure for cholesterol uptake. Tri[<sup>3</sup>H]oleate and [<sup>14</sup>C]cholesteryl oleate double radioactively labeled TRL-mimicking particles were synthesized by a laboratory technician (Department of Internal Medicine, Division of Endocrinology, LUMC) according to a previously published protocol.<sup>42-44</sup> Tri[<sup>3</sup>H]oleate is a triglyceride and [<sup>14</sup>C]cholesteryl oleate is a cholesteryl ester, which are both found in the core of the TRL particle (**Figure 1**). Unless otherwise specified, these particles were incubated with ApoC2 for 30 minutes at 37°C to incorporate ApoC2 in the particle surface, as ApoC2 is an essential co-factor for LPL activity. Consequently, 10  $\mu$ L of particle solution/well was added to the cell medium and cells were incubated at 37°C for 4 hours. After incubation, medium was removed and stored in Eppendorf tubes at -20°C, and the cells were washed with Dulbecco's phosphate buffered saline (DPBS, Gibco) and heparin solution to

remove remaining particles outside of the cells. For every group, one well was not washed with heparin as a control for the effect heparin treatment. Then, 0.1M NaOH was added to solubilize the cells. Cell lysates were transferred to counting tubes and radioactivity was counted in Ultima Gold (PerkinElmer) by a  $\gamma$ -counter. See **Appendix Expanded Methods A.3** for the detailed protocol.

The ratio between  $^3\text{H}$  and  $^{14}\text{C}$  counts was calculated. This ratio gives an indication of whole particle uptake versus free fatty acid uptake alone. Based on the particle composition a  $^3\text{H}/^{14}\text{C}$  ratio of around ten indicates whole particle uptake by the cells, while a ratio above ten indicates specific extraction of free fatty acids from the particles due to LPL activity and consequent sole free fatty acid uptake by the cells. In the physiological *in vivo* situation, not the whole particle is taken up, but only the free fatty acids from the core of this particle, by the action of LPL. After the lipoprotein particle has delivered most of its fatty acids to peripheral tissues it returns back to the liver for recycling.<sup>45</sup> Therefore, a ratio above ten indicated physiological fatty acid uptake.

## 2.4 LPL activity in the medium

Cells were incubated with heparin solution (2U/mL) for 45 minutes at 37°C to release all active LPL from the cell surface into the medium. After incubation, medium was collected in Eppendorf tubes and stored at -20°C until further analysis. See **Appendix Expanded Methods A.4** for the full protocol. A laboratory technician (Department of Internal Medicine, Division of Endocrinology, LUMC) performed an LPL activity assay on these medium samples according to an in-house protocol that is comparable to a previously published protocol.<sup>46</sup> In short, TRL-mimicking particles with incorporated radiolabeled tri[ $^3\text{H}$ ]oleate (triglyceride) were added to the medium samples, and the generation of [ $^3\text{H}$ ]oleates (free fatty acids) was quantified by counting the radioactivity in Ultima Gold (PerkinElmer) by a  $\gamma$ -counter. Background radioactivity was subtracted from medium measurements. LPL activity was measured as triglyceride hydrolase activity, and expressed as the amount of free fatty acids released per hour per mL of medium ( $\mu\text{mol}/\text{h}/\text{mL}$ ).

## 2.5 RNA purification and quantitative real-time polymerase chain reaction (qRT-PCR)

Cells were lysed and stored in a buffer (see **Appendix Expanded Methods A.5** for the protocol), until RNA was extracted and purified using the RNeasy Mini Kit (QIAGEN) following the manufacturer's instructions. The RNA concentration ( $\text{ng}/\mu\text{L}$ ) per sample was determined with a NanoDrop spectrophotometer. cDNA was synthesized using Moloney murine leukemia virus (M-MLV) reverse transcriptase (Promega). For cDNA synthesis, the required sample volume for 200 ng or 250 ng RNA (dependent on experiment) was calculated, and thereafter  $\text{H}_2\text{O}$  was added to come to a total volume of 9  $\mu\text{L}$ . This RNA solution was added into a PCR plate together with 1  $\mu\text{L}$  of random hexamers (Promega) and incubated for 10 minutes at 70°C and cooled back to 4°C with a CFX96 PCR Machine (Bio-Rad). Consequently, 10  $\mu\text{L}$  of a prepared

mastermix, which was composed of 4  $\mu$ L M-MLV buffer (Promega), 0.5  $\mu$ L M-MLV reverse transcriptase (Promega), 0.5  $\mu$ L RNasin ribonuclease inhibitor (Promega), 1.25  $\mu$ L dNTPs mix of deoxynucleotide triphosphates (Promega), and 3.75  $\mu$ L H<sub>2</sub>O, was added to each sample on the PCR plate. As a negative control a mastermix was prepared without M-MLV reverse transcriptase and RNasin ribonuclease inhibitor (-RT). The plate was incubated for 10 minutes at 25°C, 50 minutes at 45°C and 10 minutes at 70°C and hold at 4°C with a CFX96 PCR Machine (Bio-Rad) to form the cDNA. The final concentration of cDNA was 200 ng/20  $\mu$ L or 250 ng/20  $\mu$ L.

qRT-PCR was performed for target genes encoding for *LPL*, *GPIHBP1*, *CD36*, and endothelial lipase (*LIPG*). It was challenging to select a gene that could be used as housekeeping gene for both cardiomyocyte and endothelial cells, since a valid housekeeping gene should have stable expression between different experimental groups, thus in this case between different cell types. A valid housekeeping gene is crucial to normalize the gene-of-interest messenger RNA (mRNA) expression data for inherent differences in mRNA expression levels between experimental groups. Therefore, four housekeeping genes were tested to select the most stable:  $\beta$ 2-microglobulin (*Beta2*), LDL receptor related protein 10 (*LRP10*), ribosomal protein L37a (*RPL37A*), and ribosomal protein lateral stalk subunit P0 (*RPLP0*). Human gene primers for *GPIHBP1*, *CD36*, *LIPG*, *RPL37A* and *RPLP0* were not in laboratory stock, and were therefore designed using the NCBI gene database (<https://www.ncbi.nlm.nih.gov/gene>), see **Appendix Expanded Methods A.6** for the step-by-step protocol. *GPIHBP1*, *CD36* and *LIPG* primers were newly designed and therefore two primers were tested to select the most stable one, while for *RPL37A* and *RPLP0* the primer sequences were used from a previously published paper.<sup>47</sup> All used primers are listed in **Table 1**. For *GPIHBP1* and *LIPG* primer design turned out to be difficult, and therefore also commercially available primers were tested (QuantiTect Primer Assay, Qiagen). Also, for *Beta2* a commercially available primer was used from the lab stock (QuantiTect Primer Assay, Qiagen).

**Table 1.** List of primers for used for qRT-PCR. Primers were designed with the NCBI gene database. Lab stock primers were designed and tested for efficiency before use. Sequences were not available (N/A) for commercially available primers.

Gene	Source	Use	Forward primer	Reverse primer
<i>LPL</i>	Lab stock	Target	TCAACTGGATGGAGGAGGAGT	CAGGAGAAAGACGACTCGGG
<i>GPIHBP1</i>	Designed	Target	CACGGGAACACCGAGTCA	CTGGACTGGCAGCAGGTCAT
<i>GPIHBP1</i>	Designed	Target	TGGAGGGGACCCAGTGATGA	AGGCAGTGACTTCTGTCCG
<i>GPIHBP1</i>	Commercial	Target	N/A	N/A
<i>CD36</i>	Designed	Target	GCTGTTGATTTGTGAATAAGAACCA	CCTGTTTCTTGCAAACCTCTGG
<i>CD36</i>	Designed	Target	TGCTGTTGATTTGTGAATAAGAACC	AGCACCTGTTTCTTGCAAACCTC
<i>LIPG</i>	Designed	Target	GCTGCAGGAGAAGGACGATT	CCTTTCACGAAGTTGCCTGC
<i>LIPG</i>	Designed	Target	TTCACGGATGGACGATGAGC	GGAGCCAGTCAACCACAACCT
<i>LIPG</i>	Commercial	Target	N/A	N/A
<i>Beta2</i>	Lab stock, commercial	Housekeeping	N/A	N/A
<i>LRP10</i>	Lab stock	Housekeeping	CAGACTGTCACCATCAGGTTC	GAGAGGGGAGCGTAGGGTTA
<i>RPL37A</i>	Designed	Housekeeping	GTGGTTCCTGCATGAAGACAGTG	TTCTGATGGCGGACTTTACCG
<i>RPLP0</i>	Designed	Housekeeping	CACCATTGAAATCCTGAGTGATGT	TGACCAGCCCAAAGGAGAAG

For, qRT-PCR a work solution of 10  $\mu\text{L}$  forward primer, 10  $\mu\text{L}$  reverse primer and 80  $\mu\text{L}$   $\text{H}_2\text{O}$  was prepared, and consequently, a mastermix was made from 0.5  $\mu\text{L}$  primer work solution, 5  $\mu\text{L}$  SYBR green (Promega) and 0.5  $\mu\text{L}$  water (no  $\text{H}_2\text{O}$  in case of commercially available primers). cDNA was diluted with  $\text{H}_2\text{O}$  to a concentration of 1  $\text{ng}/\mu\text{L}$ , and consequently 4  $\mu\text{L}$  of cDNA and 6  $\mu\text{L}$  of mastermix were loaded into a well of a 96-well PCR plate. Plates were placed in a CFX96 PCR machine (Bio-Rad) for mRNA expression quantification, expressed as a cycle quantification value (CT). The CT value is the number of PCR cycles that is required to detect a signal from the samples. Thus, a low CT value indicates a high amount of target nucleic acid in the sample, and thus high mRNA expression. For each sample, qRT-PCR measurements were performed in duplicates.

Newly designed primers were tested for target gene amplification efficiency by determining the CT values in a four-times serial dilution of cDNA in the concentrations 4  $\text{ng}/\mu\text{L}$ , 1  $\text{ng}/\mu\text{L}$ , 0.25  $\text{ng}/\mu\text{L}$  and 0.06  $\text{ng}/\mu\text{L}$ . Efficient primers show a 2-point increase in CT value for every four-times dilution of cDNA concentration, as well as a tight melting curve.

mRNA expression was expressed as fold change compared to a different cell type using the  $\Delta\Delta\text{CT}$  method. With the  $\Delta\Delta\text{CT}$  method the CT values of the sample are compared to housekeeping genes to minimize the influence of biological differences in expression between compared samples. Mean CT values of duplicates were used for calculations. First, for each sample the  $\Delta\text{CT}$  value is calculated as the difference between the CT value of the housekeeping gene and gene of interest. One experimental group is selected as reference group, and the mean  $\Delta\text{CT}$  value is calculated from all samples in this reference group. Consequently, the  $\Delta\Delta\text{CT}$  is calculated for each sample as the  $\Delta\text{CT}$  value of that sample minus the mean  $\Delta\text{CT}$  of the reference group, and thereafter the mean  $\Delta\Delta\text{CT}$  value is calculated from all samples in each experimental group. The relative mRNA expression is now calculated for every experimental group as  $2^{(\text{mean } \Delta\Delta\text{CT})}$ , with corresponding standard deviation. Cardiomyocytes were used as the references group.

## 2.6 Western blotting

LPL protein content in the medium was determined by Western blotting. One day before medium collection, 0.5 mL of the total of 1 mL medium was removed from the cell cultures to increase the protein concentration. After, the 0.5 mL medium was collected from the cell cultures and stored at  $-20^\circ\text{C}$  until further analysis. For Western blotting, medium samples were first concentrated with a centrifugal filter (Amicon Ultra-0.5 Centrifugal Filter Unit). As the LPL monomer has a molecular weight (MW) of 60 kD,<sup>48</sup> a filter with a MW cut-off (MWCO) of 30 kD was chosen, according to manufacturer's recommendations, to concentrate molecules with a MW  $>30$  kD. First, samples were diluted with NaOH (5x for cardiomyocytes, 10x for co-cultures, not diluted for endothelial cells), and protein concentration in the samples was assessed with a protein assay kit (Thermo Fisher). The required sample volume for 10  $\mu\text{g}$  protein was calculated, and thereafter radioimmunoprecipitation assay (RIPA) buffer was

added to come to a total volume of 10  $\mu\text{L}$ , plus 4  $\mu\text{L}$  of Laemli buffer. Next, samples were separated on a polyacrylamide gel (Bio-Rad) by electrophoresis and turbo-blotted on nitrocellulose membranes (Trans-blot Turbo, Bio-Rad). After, membranes were blocked for 1 hour at room temperature on a roller bank with block solution, consisting of tris-buffered saline Tween (TBST) solution with 5% non-fat dry milk (Elk). Then, the block solution was removed and membranes were incubated overnight on a roller bank with 3 mL of the primary antibody solution, i.e. 1:5000 specific LPL antibody (in house production at Wageningen University, Dept. Human Nutrition & Health) in 3 mL 5% Elk and 7 mL TBST. Next, membranes were washed with TBST and incubated for 1 hour at room temperature on a roller bank with the secondary antibody (anti-goat). Super Signal West Pico Chemiluminescent Substrate (Thermo Scientific, Rockford, USA) was used to visualize bands on the ChemiDoc<sup>TM</sup> Touch imaging system (Bio-Rad). Images were analyzed with Image lab software (Bio-Rad).

## 2.7 Statistics

All data are expressed as mean  $\pm$  standard error of the mean (SEM). Statistical differences between the three cell type groups were determined using independent t-test (2 groups) or one-way ANOVA (>2 groups) with Dunnett's post hoc test for between group differences. For qPCR analyses statistical differences were determined with one-way ANOVA with Tukey-Kramer's post hoc test. A p-value < 0.05 was considered statistically significant. Analyses were performed with Graphpad Prism and with Excel for qRT-PCR analyses.

## 2.8 Chip design

After finding the optimal cell culturing conditions for functional LPL activity *in vitro*, the ultimate goal of the overall project is to culture cardiomyocytes as a 3D tissue that is covered by endothelial cells to mimic the real human situation as close as possible. The research group at the UT had already designed a microfluidic chip that shapes cardiomyocytes into a 3D configuration and places them into direct contact with a monolayer of endothelial cells that line a microfluidic channel (**Figure 8**). As the cardiomyocytes will start contracting they should be held in place to prevent them from getting loose and floating away. By the hourglass-like shape of the space where the cells are implemented, they are kept in space (**Figure 8.C**). The 3D tissue is implemented on the chip by encapsulating cardiomyocytes in fibrinogen and thrombin, and insert them in the top holes of the chip. The thrombin converts fibrinogen into a fibrin gel, holding the cells in place. Over a period of 5 days the cardiomyocytes degrade the fibrin and form a beating cardiac tissue. Afterwards, endothelial cells are seeded on the ceiling of the microfluidic channel.

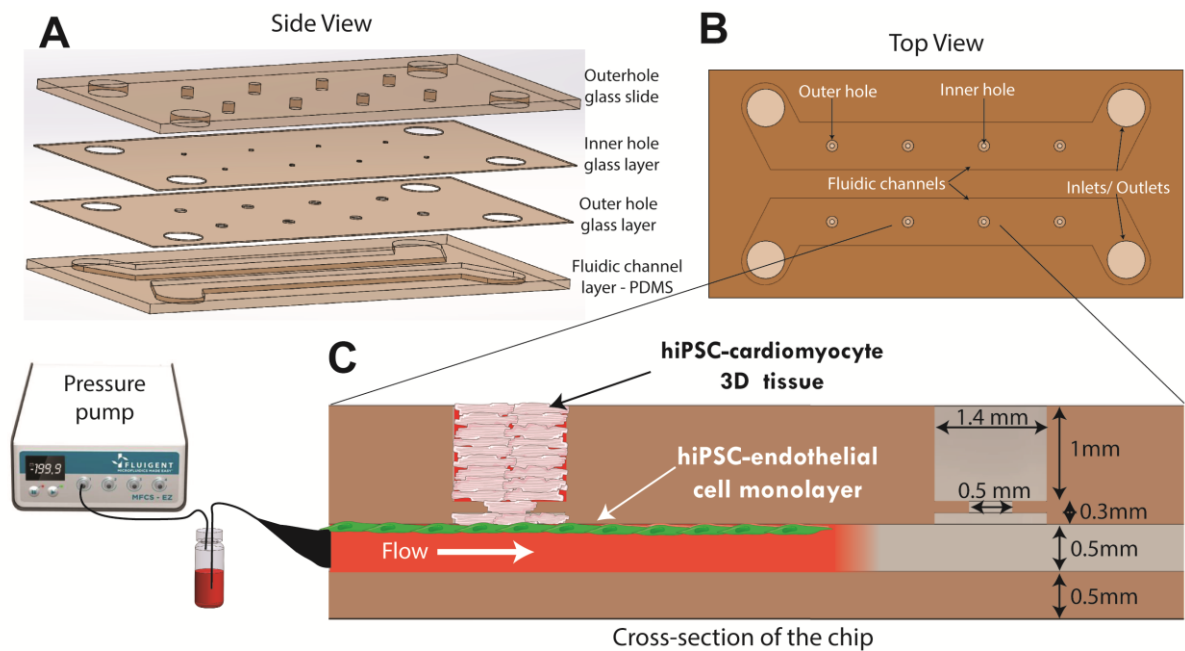


**Figure 8. Design of the heart-on-chip made out of glass.** (A) Microfluidic chip made of a glass slide and two glass coverslips, glued together with biocompatible glue, and a polydimethylsiloxane (PDMS) layer containing the fluidic channels glued to the glass by plasma bonding. The holes in the glass are made with glass drill bits. (B) Top view. (C) Sideview: 3D cardiomyocyte tissue is assembled in the holes, and in direct contact with an endothelial cell monolayer seeded on the ceiling of the microfluidic channel. Using a high-resolution pressure pump, pressure and flow is regulated in the microfluidic channels.

The problem of the current chip design is that the 3D tissue cannot be removed from the chip, as any modulation of the tissue will break the glass and damage the tissue. However, for imaging purposes it is important that the tissue can be removed intact, for embedding, sectioning and staining. Imaging of the 3D structures on the chip using confocal microscopy, is too challenging as the thickness and density of the tissue interferes with the light path emitted by the fluorophores. Therefore, the chip has to be fabricated from polydimethylsiloxane (PDMS) instead of glass making it possible to remove the tissue from the chip without damaging the 3D structure. With PDMS it may also be possible to embed and section the chip together with the tissue and then proceed with histological protocols.

For the current project, a mold for the PDMS chip was designed with Solidworks and dimensions from the glass chip were adjusted to enable removal of the PDMS from the mold without damage. The mold was made out of poly(methyl methacrylate) (PMMA) and composed of two separate halves that were fabricated with a milling machine (Datron Neo). PDMS was fabricated by thoroughly mixing curing agent to PDMS base in a 1:10 ratio, and degassing the solution for 30 minutes. Both molds were held together by clamps before PDMS was injected. The PDMS chip was cured overnight inside the mold at 71°C. After curing, the PDMS chip was removed from the mold and both the channel side of the chip as well as a 2 mm thick rectangle of PDMS were plasma treated (PDC-002-HP, Harrick Plasma) to sterilize and functionalize their surfaces, by making them temporarily hydrophilic through the insertion of polar groups. Directly after plasma treatment the channels were sealed off with the 2 mm

thick PDMS rectangle. Next, the chip was chemically functionalized with (3-aminopropyl)triethoxy silane (APTES) to enhance the PDMS surface binding capacity for fibronectin, which promotes cell adhesion.<sup>49</sup> The PDMS chip was infused with a 3% (v/v) APTES solution in deionized water and incubated for 2 minutes at room temperature under nitrogen flow. After, the chip was washed with 70% ethanol and blow dried with air. In this process, APTES reacts with the hydroxyl groups that were formed during plasma treatment. Then, the chip was sterilized with ultraviolet (UV) light for 30 minutes. Cells could be seeded on the chip within 1 hour after UV treatment.

## 3. Results

### 3.1 Pilot experiment: LPL activity in the medium

To compare LPL activity in the medium between cardiomyocyte mono-cultures and cardiomyocyte-endothelial cell co-cultures, medium was collected from heparin-treated cell cultures. Collected medium was incubated with tri<sup>[3H]</sup>oleate-labeled TRL-like particles and the release of free fatty acids from these particles was measured. **Figure 9** shows the total LPL activity expressed as tri<sup>[3H]</sup>oleate (triglyceride)-derived free fatty acid release per hour per mL medium and over a time course of 4 hours, respectively. LPL activity was significantly higher in co-cultures compared to cardiomyocytes.

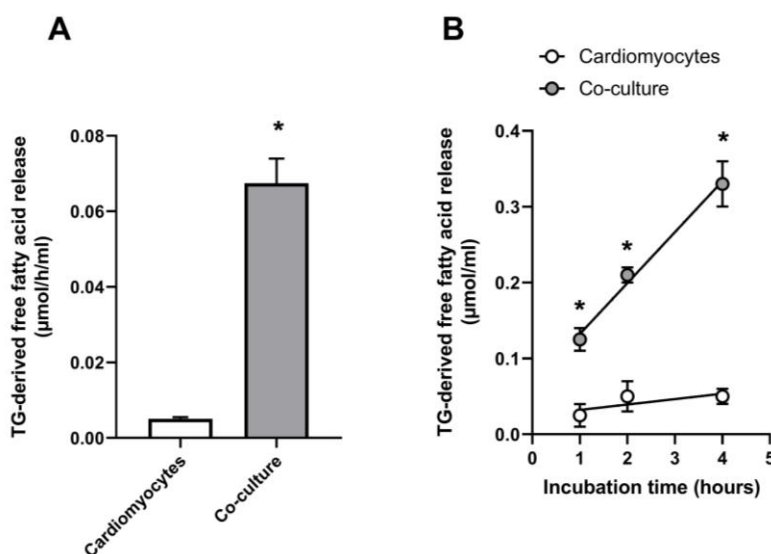


**Figure 9.** LPL activity in the medium. (A) Time-dependent release of free fatty acids derived from triglycerides of tri<sup>[3H]</sup>oleate-labeled TRL-like particles; (B) release of free fatty acids from triglycerides of tri<sup>[3H]</sup>oleate-labeled TRL-like particles in the collected medium per h/ml. Unpaired t-test was used for statistical testing. \*P<0.05 compared to cardiomyocytes (reference). TG, triglyceride.

### 3.2 Fatty acid uptake and LPL activity in different cell cultures

The pilot experiment was repeated, but now with four wells per cell culture type, and an additional group of endothelial cells in monoculture. Between the three groups (cardiomyocyte mono-cultures, cardiomyocyte-endothelial cell co-cultures, and endothelial cell monocultures) LPL activity in the medium, as well as fatty acid uptake by the cells was assessed. **Figure 10** shows optical microscopy images of the three different cell cultures. In the digital file “Supplementary movies”, the beating of the cardiomyocytes can be seen in **Movie 1** (cardiomyocytes, movie is also available via this [link](#)), **Movie 2** (co-cultures, movie is also available via this [link](#)) and **Movie 3** (co-cultures, movie is also available via this [link](#)).

LPL activity, expressed as triglyceride-derived fatty acid release, seemed to be highest in co-cultures and lowest in cardiomyocytes, although group means did not statistically significantly differ between groups (**Figure 11**). For every cell type, one well was not incubated with heparin solution before medium collection, as a negative control for heparin treatment. However, in these wells LPL activity in the medium was comparable to heparin treated cells (data not shown), indicating no effect of heparin treatment.

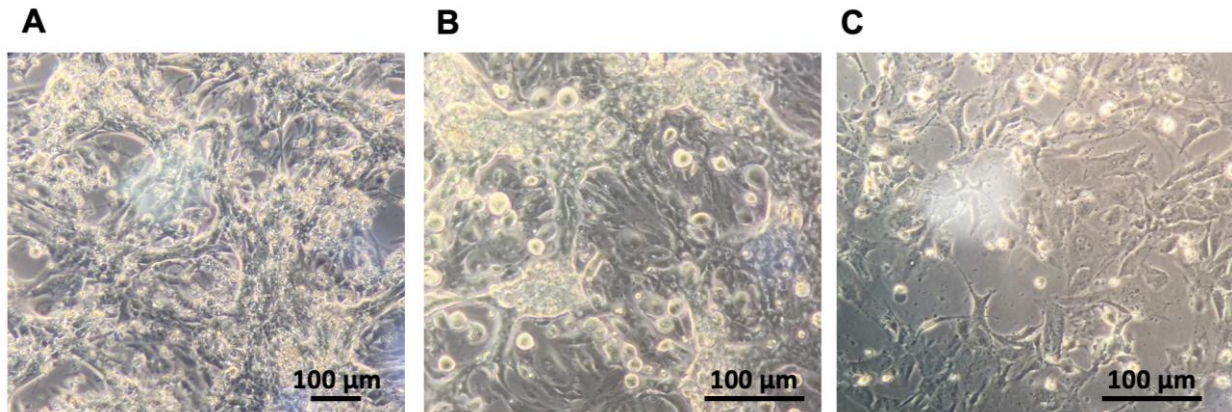


**Figure 10.** The three cell culture groups. (A) Cardiomyocyte monoculture. (B) Co-culture of cardiomyocytes and endothelial cells. (C) Endothelial cell monoculture.

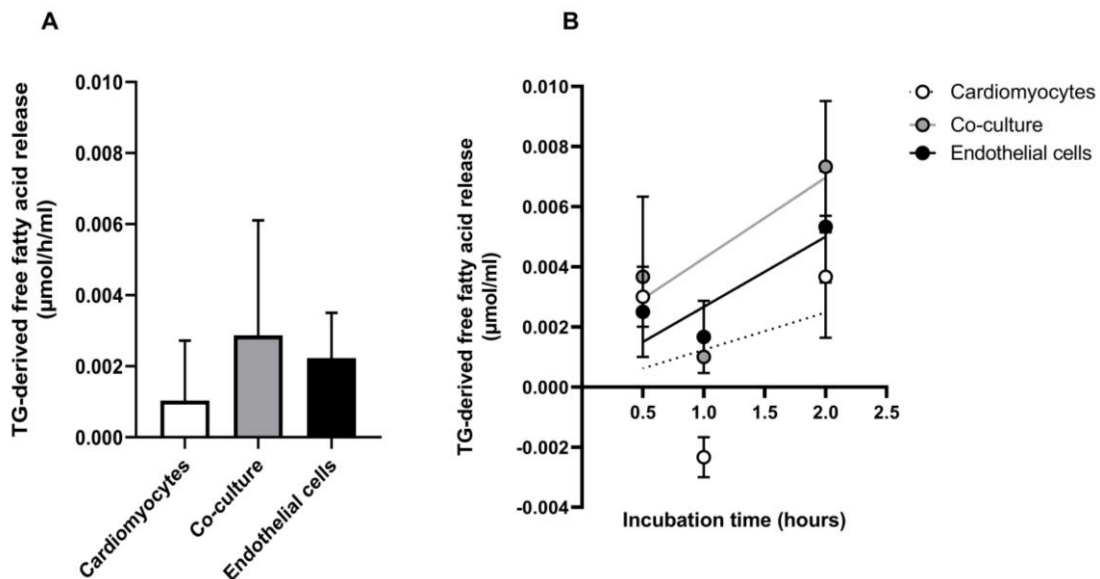


**Figure 11.** LPL activity in the medium. (A) Time-dependent release of free fatty acids derived from triglycerides of tri<sup>[3]H</sup>oleate-labeled TRL-like particles and (B) release of free fatty acids from triglycerides of tri<sup>[3]H</sup>oleate-labeled TRL-like particles in the collected medium per h/ml, in cardiomyocytes, co-cultures and endothelial cells. Values represent mean ± SEM. N is number of wells: N=3 per time point per cell culture group. One-way ANOVA was used for statistical testing. TG, triglyceride; TRL, triglyceride rich lipoprotein.

Fatty acid uptake by the different cell cultures, grouped by treatment with ApoC2 and/or heparin, is shown in **Figure 12.A**. Although not statistically significant, ApoC2 treatment tended to increase fatty acid uptake in cardiomyocytes and co-cultures, and endothelial cells

tended to have lowest fatty acid uptake. In all cell types, the ratio between fatty acid and cholesterol uptake by the cells was around 10 (**Figure 12.B**), which indicates mainly non-physiological whole particle uptake rather than specific fatty acid uptake.

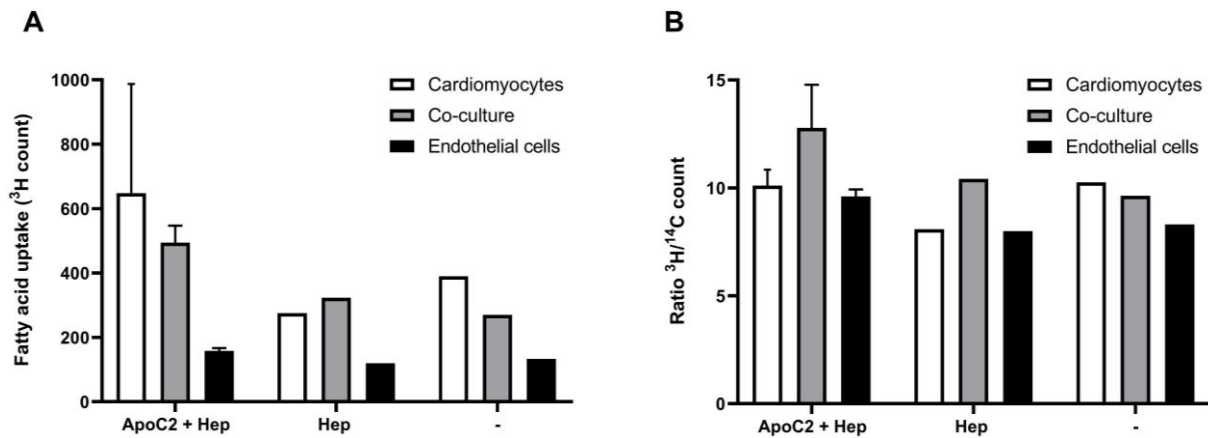


**Figure 12. Fatty acid uptake by the cells.** Cells were incubated with tri[<sup>3</sup>H]oleate and [<sup>14</sup>C]cholesteryl oleate double labeled TRL-like particles and pre-treated with ApoC2 and washed with heparin (ApoC2+Hep), not pretreated with ApoC2 and washed with heparin (Hep), or not pretreated with ApoC2 and not washed with heparin (-). **(A)** Cellular uptake of fatty acids (<sup>3</sup>H count) and **(B)** uptake ratio of <sup>3</sup>H versus <sup>14</sup>C in cardiomyocytes, co-cultures and endothelial cells. Values represent mean ± SEM. N is number of wells: N=2 per cell culture group in the ApoC2+Hep group; N=1 per cell culture group in the Hep and - groups. One-way ANOVA was used for statistical testing. ApoC2, apolipoprotein C2; Hep, heparin; TRL, triglyceride rich lipoprotein.

Cell lysates were collected to analyze mRNA expression of *LPL*, *CD36* and *GPIHBP1*, which are the genes encoding for the key proteins involved in LPL-dependent fatty acid uptake. Besides, as triglyceride hydrolase activity in the medium of endothelial cells was relatively high (**Figure 11**) compared to cardiomyocytes, mRNA expression of *LIPG* was also assessed. The *LIPG* gene encodes for the endothelium derived enzyme endothelial lipase, which can also hydrolyze triglycerides into free fatty acids similar to LPL.<sup>50,51</sup> For qRT-PCR analyses, firstly, primer efficiency was tested by a 4-times dilution series, as shown in **Figure 13**. Efficient primer gene amplification is indicated by a 2-point increase CT value with every 4-times dilution. Only primers for *CD36* and *RPLP37A* (housekeeping) showed to be efficient and could be used for further qRT-PCR analysis. Therefore, commercially available primers were used for *GPIHBP1* and *LIPG1*.

mRNA expression levels of *LPL* and *CD36* are shown in **Figure 14**, and corresponding CT values are given in **Supplementary table 1**. *LPL* expression did not significantly differ between groups, while *CD36* expression was lower in endothelial cells (P<0.0001). *GPIHBP1* expression was undetectable in cardiomyocytes and co-cultures, and therefore relative expression between the three groups could not be calculated (**Supplementary table 1**). The CT values of *GPIHBP1* in the endothelial cells were high, indicating very low expression. *LIPG* mRNA expression was undetectable in all cell culture groups.

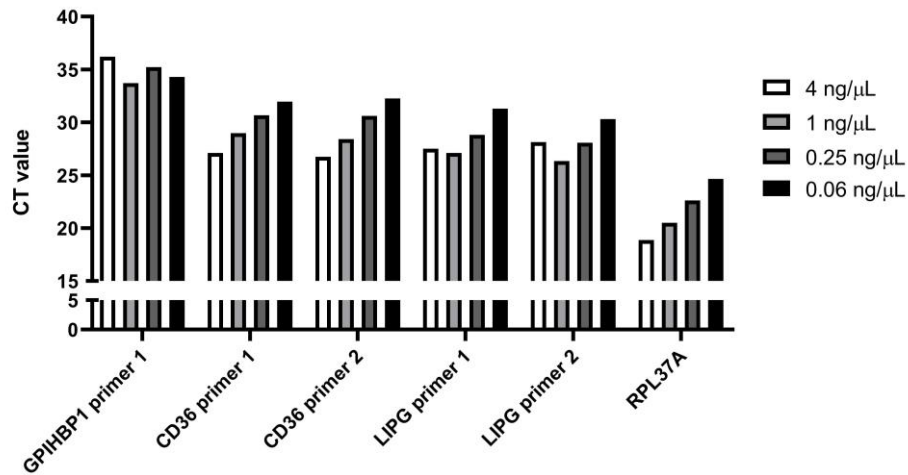


**Figure 13.** CT values for different primers a in a serial dilution of cDNA. Efficient primer gene amplification is indicated by a 2-point increase CT value with every 4-times dilution (i.e. 4 ng/μL, 1 ng/μL, 0.25 ng/μL and 0.06 ng/μL), as is the case for *CD36* and *RPL37A* primers. All measurements were performed in duplicates.

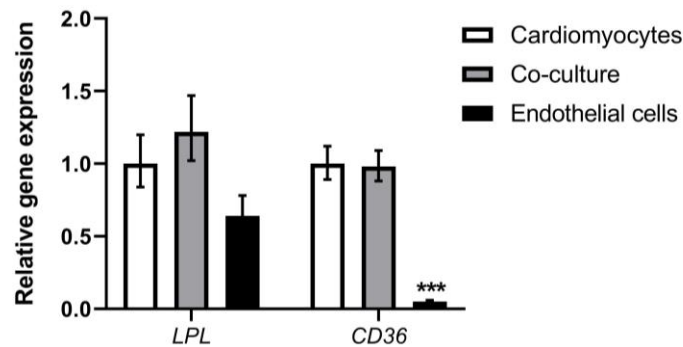


**Figure 14.** Relative mRNA gene expression of *LPL* and *CD36* determined by qRT-PCR. Expression was normalized to *RPL37A*. Values represent mean  $\pm$  SEM. N is number of wells: N=4 per cell culture group. All measurements were performed in duplicates. One-way ANOVA and Tukey-Kramer's post hoc test was used for statistical testing. \*\*\*  $P < 0.0001$  compared to cardiomyocytes (reference group).

### 3.3 Effects of particle incubation time on fatty acid uptake

In this experiment, the fatty acid uptake by the cells was assessed over a time course of 4 hours, and measured at 15, 30, 60, 120 and 240 minutes. For all groups, particles were pre-incubated with 0.05 μL/well ApoC2. As shown in **Figure 15.A**, fatty acid uptake gradually increased over time in all cell culture groups, and was maximal after 4 hours. Uptake was lower in endothelial cells compared to cardiomyocytes and co-cultures. However, fatty acid uptake did not differ between cardiomyocytes and co-cultures. The ratio between fatty acid and cholesterol uptake by the cells also increased over time for all cell types (**Figure 15.B**), and was well above ten in co-cultures after 4 hours, indicating specific fatty acid uptake rather than whole particle uptake.

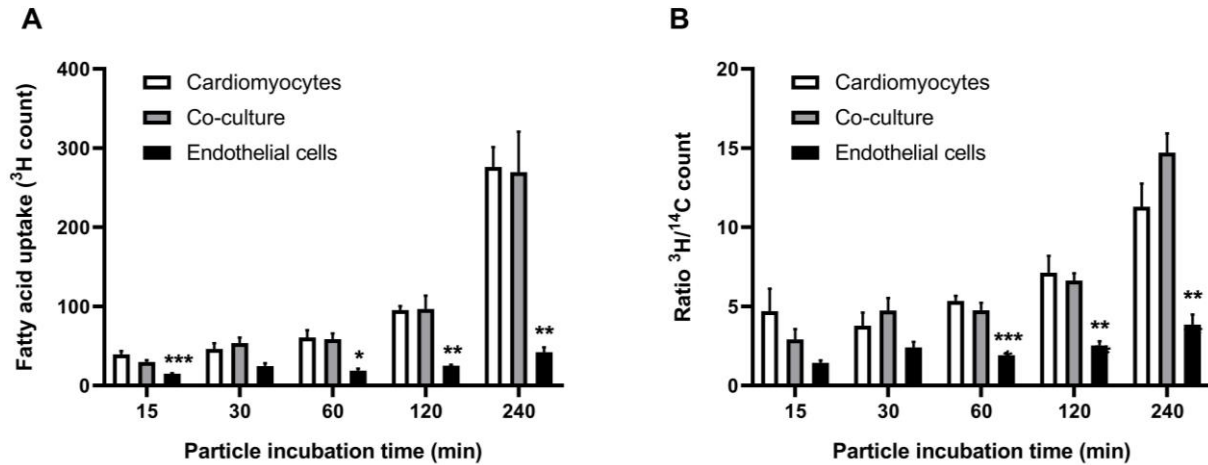


**Figure 15. Fatty acid uptake by the cells.** Cells were incubated with tri<sup>3</sup>H]oleate and [<sup>14</sup>C]cholesteryl oleate double labeled TRL-like particles for particles for 15, 30, 60, 120 or 240 minutes. **(A)** Cellular uptake of fatty acids (<sup>3</sup>H count) and **(B)** uptake ratio of <sup>3</sup>H versus <sup>14</sup>C in cardiomyocytes, co-cultures and endothelial cells. Values represent mean  $\pm$  SEM. N is number of wells: N=3 per time point for all cell culture groups. One-way ANOVA and Dunnett's post hoc test was used for statistical testing. \* P<0.05; \*\* P< 0.01; \*\*\* P<0.001 compared to cardiomyocytes (reference group).

### 3.4 Dependency of fatty acid uptake on ApoC2

In this experiment, the fatty acid uptake by the cells was assessed for different concentrations of ApoC2. Tri<sup>3</sup>H]oleate and [<sup>14</sup>C]cholesteryl oleate double labeled TRL-like particles were incubated with different concentrations of ApoC2 before they were added to the cell cultures. As shown in **Figure 16.A**, fatty acid uptake drastically increased with higher concentrations of ApoC2 in cardiomyocytes and co-cultures. Uptake was lowest in endothelial cells and seemed to be less influenced by ApoC2 concentration. The ratio between fatty acid and cholesterol uptake by the cells also increased with higher ApoC2 concentrations (**Figure 16.B**), and tripled for a concentration of 0.25  $\mu$ L ApoC2/well compared to no ApoC2, indicating specific fatty acid uptake rather than whole particle uptake.

The results shown in **Figure 16** are derived from 42-day old cardiomyocytes, counted from the start of differentiation. In **Supplementary figure 4**, results are shown for 22-day old cardiomyocytes with N=1 per concentration per cell culture group. It seemed that fatty acid uptake was consistently lower in the younger cardiomyocytes compared to the 42-day old cells.

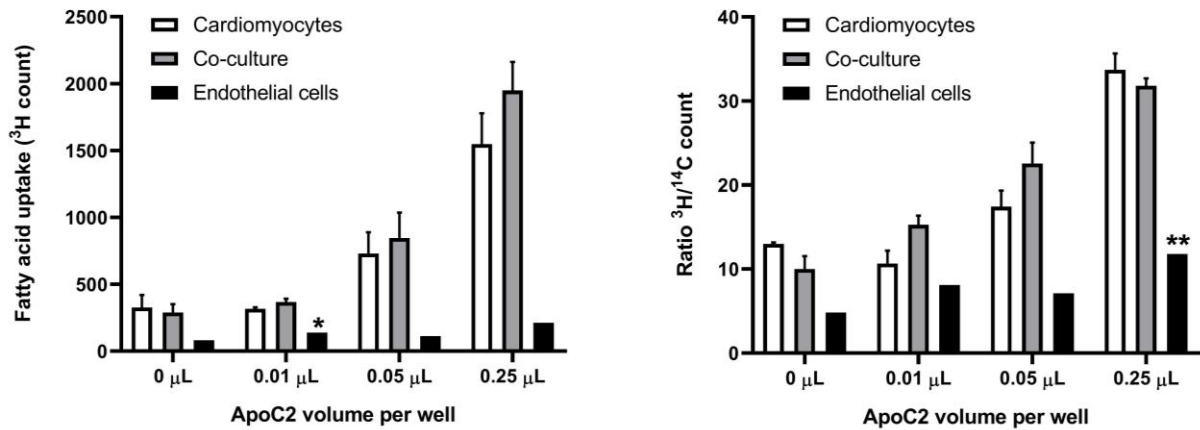


**Figure 16. Fatty acid uptake by the cells.** Cells were incubated with tri[<sup>3</sup>H]oleate and [<sup>14</sup>C]cholesteryl oleate double labeled TRL-like particles. These particles were pre-incubated with different concentrations of ApoC2, i.e. 0 μL/well, 0.01 μL/well, 0.05 μL/well or 0.25 μL/well. **(A)** Cellular uptake of fatty acids (<sup>3</sup>H count) and **(B)** uptake ratio of <sup>3</sup>H versus <sup>14</sup>C in cardiomyocytes, co-cultures and endothelial cells. Values represent mean ± SEM. N is number of wells: per concentration N=2 for cardiomyocytes, N=3 for co-cultures and N=1 for endothelial cells. One-way ANOVA and Dunnett's post hoc test was used for statistical testing. \* P<0.05; \*\* P< 0.01 compared to cardiomyocytes (reference group). ApoC2, apolipoprotein C2.

### 3.5 Presence of LPL protein in the medium

LPL protein content in the medium was determined by Western blotting. For the medium, a strong band was visible around 50 kDa (**Figure 17.A**), which is the expected height for LPL protein according to the used antibody. However, this band also appeared for medium of endothelial cells, which is not expected, as endothelial cells *in vivo* do not produce LPL. A second band was visible around 37 kDa, which seems to be mainly present in cardiomyocytes and co-cultures. The presence of multiple bands may be due to a too high amount of proteins being loaded on the gel,<sup>52</sup> since the medium samples were highly concentrated using a centrifugal filter before loading. To determine whether this was indeed the case, a negative control sample should have been taken along, consisting of only medium that had not been in contact with cells. If the Western blot of this negative control would show any similar bands, it means that the concentrated proteins in the medium itself disturb the detection of LPL. This has to be verified in future experiment. There was also no housekeeping protein used as a loading control to normalize for the level of protein in the different cell types. With the lack of a negative control and a housekeeping protein, it is not possible to properly analyze the current Western blot. Western blotting should be repeated in future experiments to draw any conclusions.

It should be noted that this experiment was meant as a try-out to check whether the available LPL antibody, which was meant to detect mouse LPL, was suitable to detect LPL in the current hPSC samples, based on the fact that the LPL gene is conserved in mice and humans.<sup>53</sup> Indeed, the antibody seems suitable to use in human samples as well, as we detected bands at the proper height of around 50 kDa.

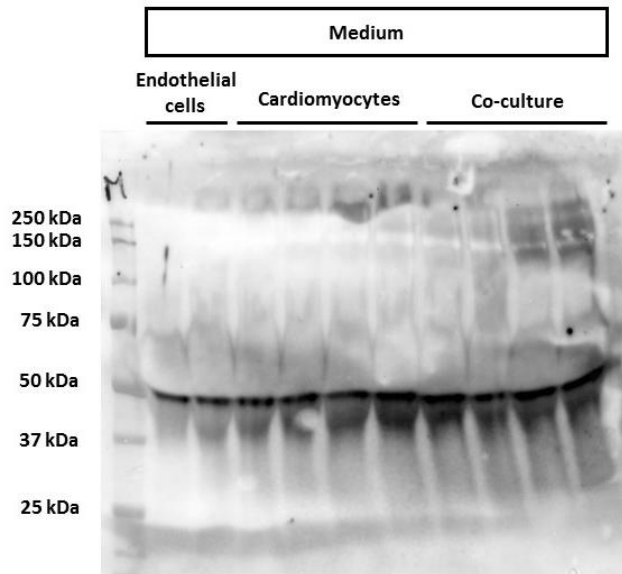


**Figure 17.** LPL protein in the medium determined by Western blotting. N=4 for all cell culture groups. For endothelial cells, medium of two wells were merged to achieve a higher protein content.

### 3.6 Chip design

The top and bottom parts of the optimal mold designs are shown in **Figure 18.A** and **Figure 18.B**. Mold design optimization was an iterative process, trying to find the smallest cylinder diameter possible that could still be milled without damage of the mold material, chipping of the mold material, irregularities of the mold material surface, or problems with the PDMS curing. Flaws in the chip design process are shown in **Supplementary figure 5**.

The top part of the optimal mold, holds three cylindric shapes with radius of 0.25 mm, 0.6 mm and 2.5 mm, respectively. As schematically illustrated in the chip cross section (**Figure 18.C**), the 0.25 mm cylinder is the thinnest part of the shape with the purpose to hold the cells in place, the 0.6 mm cylinder is 1 mm high and will hold the largest volume of cardiomyocytes, and the 2.5 mm cylinder is added to the chip to facilitate cell seeding, as a pipet tip easily fits this opening. The bottom part of the optimal mold includes the lower cylindric part of the space where the cardiomyocytes will be seeded, with a radius of 0.6 mm and height of 0.12 mm, as well as the shapes for the two microfluidic channels with a width of 5.0 mm and height of 0.5 mm. In the final PDMS chip, the area where the lower cylindric part and the channel meet is the surface of contact between the cardiomyocytes and endothelial cells, as the endothelial cells will be seeded on the ceiling of the channel.

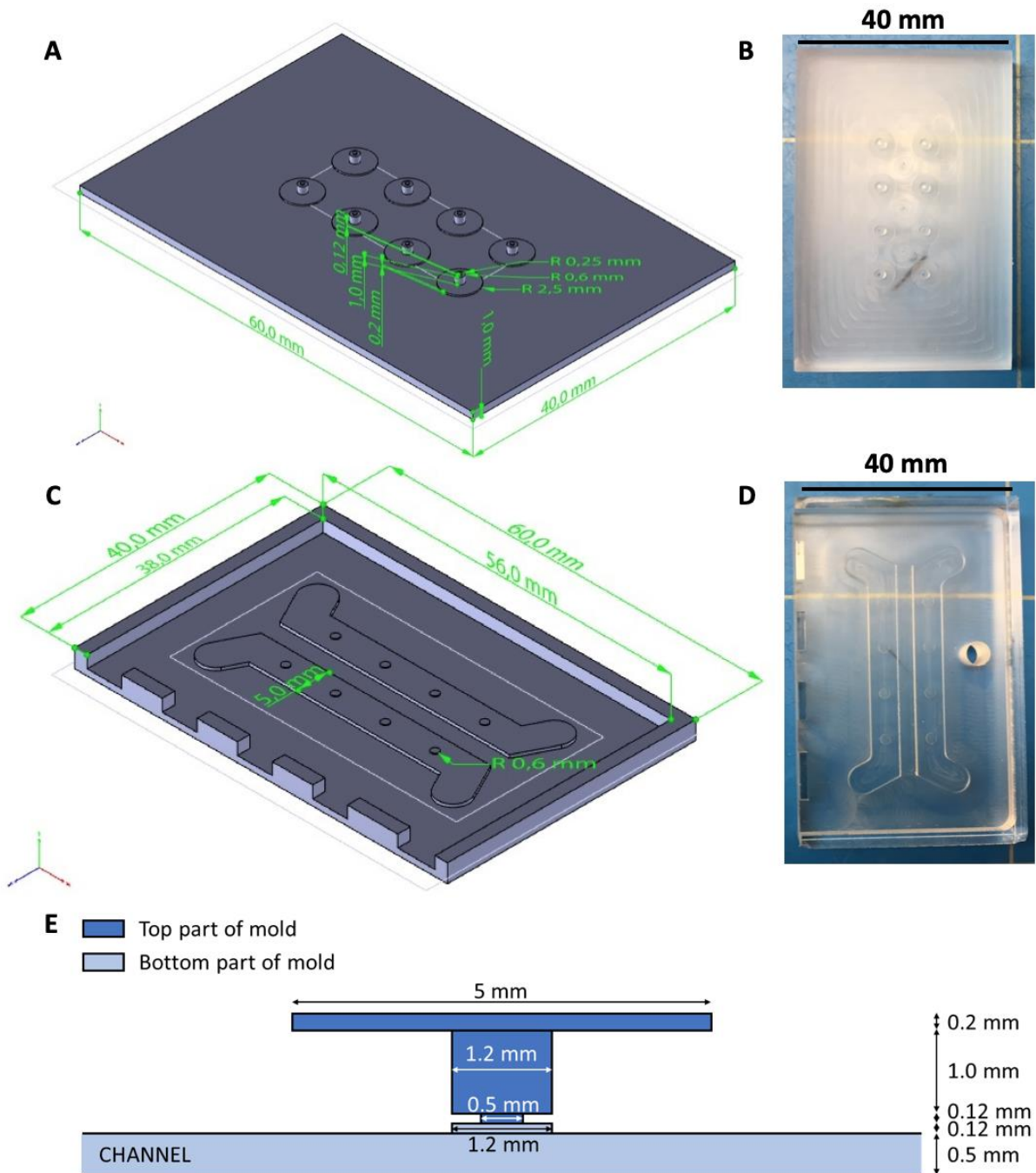


**Figure 18. Solidworks mold design.** (A) Top part of the mold. (B) Bottom part of the mold with the channels. (C) Cross section of the chip, with the spaces derived from the top mold shown in dark blue and the spaces derived from the bottom mold shown in light blue.

After mold optimization, an optimal PDMS chip was fabricated (**Figure 19.A**), which had no air bubble formation inside the PDMS, and fully connected and circular cell seeding spaces (**Figure 19.B**). After plasma treatment and chemical functionalization, cardiomyocytes were seeded on the chip to verify if they would stay in place, which was indeed the case (**Figure 19.C**). The beating cardiomyocyte tissue on the chip can be seen in **Movie 4** in the digital file “Supplementary movies”. The movie is also available via this [link](#).

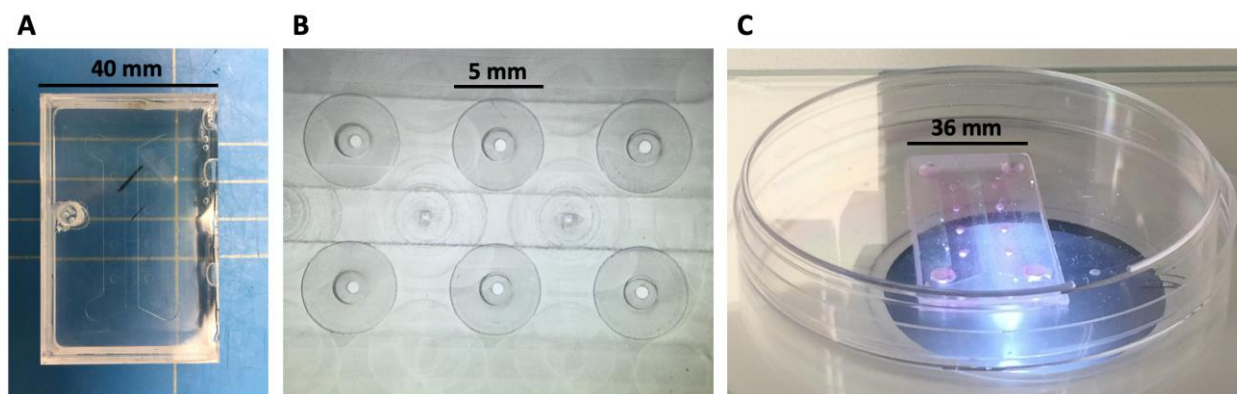


**Figure 19. PDMS chip.** (A) Cured PDMS in the mold. (B) Top view of the PDMS chip. (C) Cardiomyocytes seeded on the PDMS chip.

## 4. Discussion

In this project, the fatty acid uptake and LPL activity of hPSC-derived cardiomyocytes and endothelial cells was studied, using tri[<sup>3</sup>H]oleate (triglyceride) and [<sup>14</sup>C]cholesteryl oleate (cholesterol ester) double radioactively labeled TRL-mimicking particles. Differences between cardiomyocyte monocultures, cardiomyocyte-endothelial cell co-cultures and endothelial cell monocultures were compared to verify whether co-culturing stimulates LPL activity. LPL activity in the medium, measured as triglyceride-derived fatty acid release, was highest in co-cultures. Fatty acid uptake by the cells also seemed to be higher in co-cultures than cardiomyocyte monocultures, although differences were not statistically significant. Endothelial cells consistently showed the lowest fatty acid uptake. Importantly, incubation of TRL-mimicking particles with ApoC2, which is an essential co-factor of LPL enzymatic activity, drastically increased fatty acid uptake by cardiomyocytes and co-cultures.

Incubation of TRL-mimicking particles with ApoC2 before addition to the cell cultures leads to incorporation of ApoC2 in the particle surface.<sup>42</sup> *In vivo*, ApoC2, which is present on the surface of lipoprotein particles, is an essential co-factor for activation of LPL.<sup>54-56</sup> In line, it was shown in the current experiments that if higher concentrations of ApoC2 were added to the TRL-particles, fatty acid uptake by both cardiomyocytes and co-cultures drastically increased. This clearly indicates that fatty acid uptake is ApoC2 dependent, strongly indicating that fatty acid uptake is mediated via LPL-induced hydrolyses of the radiolabeled triglycerides (tri[<sup>3</sup>H]oleates) in the TRL-particles. Fatty acid uptake was highest with addition of 0.25 μL/well of ApoC2, which was the highest concentration used in the experiments. Compared to a 5-times lower ApoC2 concentration (0.05 μL/well), fatty acid uptake nearly doubled. Even higher concentrations of ApoC2 may lead to even higher fatty acid uptake. Interestingly, with increasing ApoC2 concentrations, the difference in fatty acid uptake between cardiomyocytes and co-cultures tended to increase, with co-cultures showing the highest fatty acid uptake. Possibly, differences between co-cultures and monocultures of cardiomyocytes only become visible when LPL is highly activated, which would require a high amount of ApoC2. To test this hypothesis, it is important to perform future experiments with even higher concentrations of ApoC2 than 0.25 μL/well. The importance of an optimal ApoC2 concentration was even further stressed by the observation that at highest ApoC2 concentration, the uptake ratio between triglycerides and cholesterol (<sup>3</sup>H/<sup>14</sup>C) was also highest, being 3 times higher compared to no ApoC2 addition (30 versus 10, respectively). This uptake ratio gives an indication of whole particle uptake versus specific free fatty acid uptake. Based on the particle composition, a <sup>3</sup>H/<sup>14</sup>C ratio of around ten indicates whole particle uptake by the cells, while a ratio above ten indicates specific extraction of free fatty acids from the particles due to LPL activity, and consequent sole free fatty acid uptake by the cells. Addition of ApoC2 increased the specific free fatty acid uptake by the cells (high <sup>3</sup>H/<sup>14</sup>C ratio), while in the absence of ApoC2 it seems that only whole particles are taken-up (low <sup>3</sup>H/<sup>14</sup>C ratio). This is fully in line with LPL

physiology, since in the physiological *in vivo* situation, where ApoC2 is present on lipoprotein surfaces, not the whole particle is taken up, but only the free fatty acids from the core of this particle, as mediated by the action of LPL. It thus seems that ApoC2 is crucial to mimic physiological fatty acid uptake *in vitro*.

In line with the ApoC2 data, *LPL* gene expression tended to be highest in co-cultures, followed by cardiomyocytes, while being lowest in endothelial cells. However, it should be noted that gene expression data were obtained from cell cultures that were not incubated with ApoC2. It may be possible that *LPL* gene expression is further upregulated in response to the presence of ApoC2. As LPL regulation occurs for a large part post-transcriptionally, gene expression levels may not be one-to-one linked to protein levels.<sup>12,57</sup> Unfortunately, it was not possible to gain any concluding results from the Western blot. Gene expression of *GPIHBP1* and *CD36* were also determined, which are known to be expressed by endothelial cells.<sup>13,58</sup> Indeed, *GPIHBP1* was only expressed in endothelial cells, although expression levels were low. However, in contrast to expectations, *CD36* expression was low in endothelial cells compared to cardiomyocytes. The exact reason for this is unknown, but it could relate to the fact that hPSC-derived cells may not fully mimic *in vivo* adult cells, at least in the current culturing conditions.<sup>59</sup>

It was also shown that fatty acid uptake increases over a time course of 4 hours. Although the experiment was performed with addition of only 0.05  $\mu\text{L}/\text{well}$  ApoC2, which explains the relatively low  $^3\text{H}$  count, the increase in fatty acid uptake confirms the existence of true cellular fatty acid uptake. Despite thorough washing of the cells before the radioactivity measurement, it may still be possible that radiolabeled TRL-particles stick between the cells, showing a signal on the  $\gamma$ -counter that is not related to the biological process of fatty acid uptake by the cells ('background radioactivity'). However, the consistent increase in fatty acid uptake over time, rules out the possibility that we are just looking at 'background radioactivity'. However, from a physiological point of view, the observed consistent increase of fatty acid uptake over time is not expected. For example in mice, that were injected with the same radiolabeled TRL-particles in the blood stream, triglycerides ( $^3\text{H}$ -counts) disappear from the blood within 15 minutes,<sup>44</sup> while only 40% of the radioactive label can thereafter be traced in the organs [unpublished data Kooijman et al.], indicating that 60% of the triglycerides have been burned into  $\text{CO}_2$  and  $\text{H}_2\text{O}$  in the meantime. Therefore, it would be expected that cellular fatty acid uptake reaches a plateau phase before 4 hours, due to an equal amount of fatty acids being taking-up and being burned by the cells. The lack of such a plateau phase in the current results may indicate that the cardiomyocytes do not utilize the fatty acids as energy source, but rather store them intracellularly. Interestingly, it has previously been shown that fatty acid utilization is highly dependent on culture medium composition. More energy is generated through oxidative phosphorylation in iPSC-cardiomyocytes on a medium with galactose and fatty acids, compared to cells on a medium with glucose and fatty acids, which mainly rely on glycolysis.<sup>60</sup> It stands out that iPSC-cardiomyocytes keep a preference for glucose even in the presence of fatty acids, while they change to oxidative phosphorylation in

the presence of galactose. Apparently, addition of galactose to the medium is crucial to enhance fatty acid oxidation. Without galactose added to the fatty acid containing medium, fatty acids accumulated in the cells and cell viability diminished.<sup>61</sup> The underlying reason is that galactose is metabolized at a much slower rate than glucose, forcing cells to switch to oxidative phosphorylation, whereby they start utilizing fatty acids as well. While in a glucose-rich medium, cells preferentially utilize glucose via glycolysis and fatty acids accumulated in the cells.<sup>61</sup> This mechanism might have played a role in the present experiments, as both galactose and glucose were added to the medium. If the glucose concentration was sufficient to use glycolysis as the preferential energy source, fatty acids may be stored rather than utilized, thereby explaining the lack of a plateau phase in fatty acid uptake within 4 hours.

As endothelial cells are far less metabolically active than cardiomyocytes, their fatty acid uptake is expected to be low. Indeed, it was shown that fatty acid uptake by endothelial cells is much lower than by cardiomyocytes. However, LPL activity, expressed as triglyceride derived free fatty acid release, in the medium of endothelial cells seemed to be higher in endothelial cells than cardiomyocyte monocultures. This contradictory finding, may be explained by the fact that triglyceride derived free fatty acid release is not a direct measure of LPL activity, but rather a general measure of the lipolytic activity of the medium. Endothelial cells are known to produce the enzyme endothelial lipase encoded by the *LIPG* gene, which is able to hydrolyze triglycerides into fatty acids in a similar manner as LPL.<sup>50,51</sup> For that reason, *LIPG* gene expression was measured, however, expression was undetectable in all cell cultures, and does probably not explain this finding. Another explanation for the relatively high lipolytic activity in the endothelial cell medium was not yet found, and should be studied in more detail in future experiments.

Several factors have been shown to increase hPSC-cardiomyocyte maturation, of which one is long-term cell culturing.<sup>33,62</sup> Interestingly, fatty acid uptake seemed to be consistently lower in the 22 day old cardiomyocytes compared to the 42-day old cells, which would suggest that long-term culturing also increases metabolic maturation of these cells. However, the old and younger cells were derived from different differentiation batches and therefore care should be taken when interpreting the results. In a future experiment, it would be interesting to compare fatty acid uptake between cells from different ages, which are derived from the same differentiation badge.

In the fatty acid uptake assay, heparin was used to wash away any remaining TRL-mimicking particles between the cells before counting the radioactivity in the  $\gamma$ -counter. Heparin treatment did not change fatty acid uptake in any of the cell types. This seems to indicate that all particles were already washed away with DPBS, and heparin treatment did not have an additional effect. This would indicate that standard treatment of cells with heparin is not necessary in future experiments. However, the number of wells per group was low, and therefore it is recommended to repeat experiments with higher statistical power to draw solid conclusions.

It should be noted that the performed experiments had low statistical power due to small group sizes, which resulted in a reduced chance of detecting a true effect. As a consequence, we may not have succeeded to show statistically significant differences between cardiomyocyte and co-culture groups, although true differences may have been present. Since effect sizes were all in the expected (biological) direction, there is reason to assume that we are looking at true effects. These experiments are therefore important indicators to proceed with this project. However, follow-up experiments have to be performed with larger group sizes to convincingly show differences between groups.

Noteworthy, the cardiomyocyte populations used in this study were not 100% pure cardiomyocytes, due to the non-optimal differentiation of hPSC. It is estimated that 75-85% of the total cell populations were cardiomyocytes [unpublished data Ribeiro et al.]. During differentiation, part of the hPSC differentiates to other cells types than cardiomyocytes, such as endothelial cells, fibroblasts or cells with an intermediate phenotype. Since the non-cardiomyocytes form a relatively small amount of the total population, it is expected that these cells do not influence the results to a substantial extent. However, since the effects of co-culturing cardiomyocytes with endothelial cells are of main interest in this project, it would be optimal to work with pure cardiomyocyte populations in follow-up experiments. This could be achieved by using single cell sorting to derive pure cardiomyocyte populations.

The current experiments were all performed in a 2D setting on culturing plates, mainly as a form of pilot experiments and to define optimal culturing and experimental conditions. However, the past few years multiple studies by different academic groups have established the superiority of 3D iPSC cardiac models over 2D cardiac models, as 3D cardiac models show a closer resemblance to the human adult heart in morphology, electrophysiology and functionality.<sup>63-65</sup> More recently, it was shown that a 3D configuration of human iPSC-cardiomyocytes also improves metabolic maturation compared to 2D cell cultures, showing a higher reliance on fatty acid oxidation rather than anaerobic glycolysis, in line with an increased mitochondrial mass, DNA and protein content.<sup>66,67</sup> One of the most important difference that distinguishes 3D human iPSC-cardiomyocyte tissue from 2D cell cultures is the ability to generate contractile force and tension in a 3D setting. The pharmacological inhibition of this contractility by a myosin II inhibitor led to decreased mitochondrial DNA and mass, which implies that the contractile work load of 3D heart tissue contributes to metabolic maturation.<sup>67</sup> Moreover, 3D cell-to-cell interactions and the complex architecture of the human heart, which is build out of different cell types, are impossible to mimic in 2D models. Since the ultimate aim of the current project is to mimic the *in vivo* interaction between TRL particles in the blood, vessels covered with endothelial cells and contractile heart tissue, a 3D model is required to fulfill this aim. Therefore, a 3D heart-on-chip model was designed to mimic direct interaction between endothelial cells and cardiomyocytes, which is believed to be essential for functional LPL activity, with addition of a microfluidic channel trough which TRL-particles can be supplied to the tissue. In the current project, one test round has been performed to implement cardiomyocytes on this chip to check whether the cardiomyocytes

stayed in place, which was indeed the case. The restricted time period of this master thesis project did not allow for further testing of the chip. Follow-up experiments have to show whether seeding of endothelial cells on the ceiling of the microfluidic channel will succeed, and whether functional LPL activity can be assessed in this way.

## 5. Conclusion

In conclusion, the results of the current experiments strongly indicate that co-culturing cardiomyocytes with endothelial cells, compared to mono-culturing, increases fatty acid uptake by the cells and triglyceride-derived free fatty acid release in the cell culture medium. Both increased cellular fatty acid uptake and triglyceride-derived free fatty acid release in the cell culture medium are indicators of functional LPL activity. Importantly, ApoC2, which is an essential co-factor of LPL enzymatic activity, drastically increased fatty acid uptake by cardiomyocytes and co-cultures. This is strong evidence that the observed increase in fatty acid uptake is indeed a consequence of increased LPL activity. Optimal LPL activity was achieved by incubating TRL-mimicking particles with at least 0.25  $\mu\text{L}$ /well ApoC2, at a particle incubation time of 4 hours. It is recommended to perform future experiments under these conditions, with the note of using a larger number of replicates per group.

The results of the current project showed that it seems possible to mimic functional LPL activity *in vitro* using hPSC-derived cells, which is of high importance for the development of pre-clinical drug screening assays targeted at LPL activation. Based on the promising results of this project, it is recommended to proceed with the development of a 3D heart-on-chip model that mimics human *in vivo*-like endothelial-cardiomyocyte interaction, in order to create a fully functional model for LPL activity *in vitro*.

## 6. Future considerations

During my master thesis project, I have been involved in writing an application for the Health~Holland Organ-on-chip Showcases (HHOCS) grant, named “*LIP@HEART: Functional lipoprotein lipase expression and modulation using heart-on-chip technology: towards a novel screening system for lipid-lowering therapy*”. The proposed project is a collaborative project between the UT (Prof. dr. Robert Passier and Dr. Marcelo Ribeiro) and LUMC (Prof. dr. Patrick Rensen and Dr. Lisanne Blauw). In short, our project aims to develop a heart-on-chip screening platform for the identification of novel drugs that lower the risk of cardiovascular disease by activating the enzyme LPL. We were very happy to receive the good news in July that the project was granted (<https://www.lumc.nl/over-het-lumc/nieuws/2019/Juli/organ-on-a-chip/>, <https://www.health-holland.com/project/2019/heart-on-chip-technology-as-a-novel-screening-system-for-lipid-lowering-therapy>). From September 2019, I will be appointed as a postdoctoral researcher at the UT to work fulltime on this project.

Based on the outcomes of this master thesis project, several considerations for future experiments should to be taken into account. First of all, in the performed experiments there was no correcting made for cell count. To make a better comparison between cardiomyocyte monocultures and cardiomyocyte endothelial cell co-cultures, we will separate the endothelial cells from the cardiomyocytes by immunomagnetic selection using anti-CD31 antibody-coupled magnetic beads, according to a previously published protocol.<sup>41</sup> Afterwards, it will be possible to count the radioactivity in the separated cardiomyocytes, in order to directly compare them to cardiomyocytes from monocultures. Secondly, it is important to use pure cardiomyocytes populations in follow-up experiments, as discussed above. Thirdly, we will change the medium composition to a medium that is more suitable for cardiomyocyte maturation, by trying to change the ratio between glucose and galactose. The challenge is that co-culturing demands for a medium that thrives both cardiomyocytes as well as endothelial cells. Thirdly, functional LPL is a dimer, which falls apart in inactive monomers and loses its enzymatic activity when it is not bound to endothelial cells.<sup>18-20</sup> It would therefore be highly interesting to make a Western blot for the LPL monomer and dimer separately. Moreover, gene expression patterns and cardiomyocyte maturation status should be studied in more detail.

# Acknowledgements

I would like to gratefully acknowledge Marcelo Ribeiro for the perfect supervision, Hetty Sips and Aisen de Sá Vivas for patiently teaching me all the skills I gained during this project, and Iulian Apachitei for his valuable advice. I thank Robert Passier, Patrick Rensen, Jimmy Berbée and Sander Kooijman for the fruitful collaboration and supervision, Simone ten Den and Kim Vermeul for the delivery of all cells used for this project, and Trea Streefland for the technical support. I thank Amanda Hagenaar-Pronk, Enchen Zhou and Cong Liu for the provision of TRL-labelled particles. Furthermore, I would like to thank Eline Kuipers for helping me out with the qRT-PCR and Wietse in het Panhuis for providing the antibodies for Western blotting. And of course, I would like to thank all my colleagues at UT and LUMC for the great time I had during my internship.

Finally, I gratefully thank Iulian Apachitei, Peter-Leon Hagedoorn, Tim Horeman, Marcelo Ribeiro and Amir Zadpoor for taking seat in my examining committee.

# References

1. WHO. Cardiovascular Diseases Fact Sheet. [http://www.who.int/news-room/fact-sheets/detail/cardiovascular-diseases-\(cvds\)](http://www.who.int/news-room/fact-sheets/detail/cardiovascular-diseases-(cvds)). 2016.
2. Global, regional, and national age-sex specific mortality for 264 causes of death, 1980-2016: a systematic analysis for the Global Burden of Disease Study 2016. *Lancet (London, England)* 2017; **390**(10100): 1151-210.
3. Ference BA, Ginsberg HN, Graham I, et al. Low-density lipoproteins cause atherosclerotic cardiovascular disease. 1. Evidence from genetic, epidemiologic, and clinical studies. A consensus statement from the European Atherosclerosis Society Consensus Panel. *European heart journal* 2017; **38**(32): 2459-72.
4. Reith C, Armitage J. Management of residual risk after statin therapy. *Atherosclerosis* 2016; **245**: 161-70.
5. Sabatine MS, Giugliano RP, Keech AC, et al. Evolocumab and Clinical Outcomes in Patients with Cardiovascular Disease. *The New England journal of medicine* 2017; **376**(18): 1713-22.
6. Weintraub WS, Gidding SS. PCSK9 Inhibitors: A Technology Worth Paying For? *PharmacoEconomics* 2016; **34**(3): 217-20.
7. Nordestgaard BG, Varbo A. Triglycerides and cardiovascular disease. *The Lancet* 2014; **384**(9943): 626-35.
8. Nordestgaard BG. Triglyceride-Rich Lipoproteins and Atherosclerotic Cardiovascular Disease: New Insights From Epidemiology, Genetics, and Biology. *Circulation research* 2016; **118**(4): 547-63.
9. Varbo A, Nordestgaard Børge G. Remnant Cholesterol and Triglyceride-Rich Lipoproteins in Atherosclerosis Progression and Cardiovascular Disease. *Arteriosclerosis, Thrombosis, and Vascular Biology* 2016; **36**(11): 2133-5.
10. Varbo A, Benn M, Tybjaerg-Hansen A, Jørgensen AB, Frikke-Schmidt R, Nordestgaard BG. Remnant Cholesterol as a Causal Risk Factor for Ischemic Heart Disease. *Journal of the American College of Cardiology* 2013; **61**(4): 427-36.
11. Engelking LR. Textbook of Veterinary Physiological Chemistry (Third Edition), <https://www.sciencedirect.com/topics/medicine-and-dentistry/lipoprotein>. 2015.
12. Goldberg IJ, Eckel RH, Abumrad NA. Regulation of fatty acid uptake into tissues: lipoprotein lipase- and CD36-mediated pathways. *Journal of lipid research* 2009; **50** Suppl: S86-90.
13. Beigneux AP, Davies BSJ, Gin P, et al. Glycosylphosphatidylinositol-Anchored High-Density Lipoprotein-Binding Protein 1 Plays a Critical Role in the Lipolytic Processing of Chylomicrons. *Cell Metabolism* 2007; **5**(4): 279-91.
14. Santamarina-Fojo S, Dugi KA. Structure, function and role of lipoprotein lipase in lipoprotein metabolism. *Current opinion in lipidology* 1994; **5**(2): 117-25.
15. Olivecrona G, Olivecrona T. Triglyceride lipases and atherosclerosis. *Current opinion in lipidology* 2010; **21**(5): 409-15.
16. Eckel RH. Lipoprotein Lipase. *New England Journal of Medicine* 1989; **320**(16): 1060-8.
17. Davies BSJ, Beigneux AP, Barnes RH, et al. GPIHBP1 Is Responsible for the Entry of Lipoprotein Lipase into Capillaries. *Cell Metabolism* 2010; **12**(1): 42-52.
18. Garfinkel AS, Kempner ES, Ben-Zeev O, Nikazy J, James SJ, Schotz MC. Lipoprotein lipase: size of the functional unit determined by radiation inactivation. *Journal of lipid research* 1983; **24**(6): 775-80.
19. Osborne JC, Bengtsson-Olivecrona G, Lee NS, Olivecrona T. Studies on inactivation of lipoprotein lipase: role of the dimer to monomer dissociation. *Biochemistry* 1985; **24**(20): 5606-11.
20. Lookene A, Zhang L, Hultin M, Olivecrona G. Rapid subunit exchange in dimeric lipoprotein lipase and properties of the inactive monomer. *The Journal of biological chemistry* 2004; **279**(48): 49964-72.

21. Olkkonen VM, Sinisalo J, Jauhiainen M. New medications targeting triglyceride-rich lipoproteins: Can inhibition of ANGPTL3 or apoC-III reduce the residual cardiovascular risk? *Atherosclerosis* 2018; **272**: 27-32.
22. Rosenson RS, Davidson MH, Hirsh BJ, Kathiresan S, Gaudet D. Genetics and Causality of Triglyceride-Rich Lipoproteins in Atherosclerotic Cardiovascular Disease. *Journal of the American College of Cardiology* 2014; **64**(23): 2525-40.
23. Wolska A, Dunbar RL, Freeman LA, et al. Apolipoprotein C-II: New findings related to genetics, biochemistry, and role in triglyceride metabolism. *Atherosclerosis* 2017; **267**: 49-60.
24. Larsson M, Vorrso E, Talmud P, Lookene A, Olivecrona G. Apolipoproteins C-I and C-III inhibit lipoprotein lipase activity by displacement of the enzyme from lipid droplets. *The Journal of biological chemistry* 2013; **288**(47): 33997-4008.
25. Hato T, Tabata M, Oike Y. The Role of Angiopoietin-Like Proteins in Angiogenesis and Metabolism. *Trends in Cardiovascular Medicine* 2008; **18**(1): 6-14.
26. Schaap FG, Rensen PC, Voshol PJ, et al. ApoAV reduces plasma triglycerides by inhibiting very low density lipoprotein-triglyceride (VLDL-TG) production and stimulating lipoprotein lipase-mediated VLDL-TG hydrolysis. *The Journal of biological chemistry* 2004; **279**(27): 27941-7.
27. Pascual F, Coleman RA. Fuel availability and fate in cardiac metabolism: A tale of two substrates. *Biochimica et biophysica acta* 2016; **1861**(10): 1425-33.
28. Stanley WC, Recchia FA, Lopaschuk GD. Myocardial Substrate Metabolism in the Normal and Failing Heart. *Physiological Reviews* 2005; **85**(3): 1093-129.
29. Neely JR, Rovetto MJ, Oram JF. Myocardial utilization of carbohydrate and lipids. *Progress in Cardiovascular Diseases* 1972; **15**(3): 289-329.
30. Heineman FW, Balaban RS. Control of mitochondrial respiration in the heart in vivo. *Annual review of physiology* 1990; **52**: 523-42.
31. Malandraki-Miller S, Lopez CA, Al-Siddiqi H, Carr CA. Changing Metabolism in Differentiating Cardiac Progenitor Cells—Can Stem Cells Become Metabolically Flexible Cardiomyocytes? *Frontiers in Cardiovascular Medicine* 2018; **5**(119).
32. Lodish H, Berk A, Zipursky S. Oxidation of Glucose and Fatty Acids to CO<sub>2</sub> *Molecular Cell Biology New York: WH Freeman; Available from: <https://www.ncbi.nlm.nih.gov/books/NBK21624/>* 2000; **4th edition**(Section 16.1).
33. Machiraju P, Greenway SC. Current methods for the maturation of induced pluripotent stem cell-derived cardiomyocytes. *World journal of stem cells* 2019; **11**(1): 33-43.
34. Denning C, Borgdorff V, Crutchley J, et al. Cardiomyocytes from human pluripotent stem cells: From laboratory curiosity to industrial biomedical platform. *Biochimica et biophysica acta* 2016; **1863**(7 Pt B): 1728-48.
35. Lopaschuk GD, Jaswal JS. Energy metabolic phenotype of the cardiomyocyte during development, differentiation, and postnatal maturation. *Journal of cardiovascular pharmacology* 2010; **56**(2): 130-40.
36. Breckenridge RA, Piotrowska I, Ng KE, et al. Hypoxic regulation of hand1 controls the fetal-neonatal switch in cardiac metabolism. *PLoS biology* 2013; **11**(9): e1001666.
37. Giacomelli E, Bellin M, Orlova VV, Mummery CL. Co-Differentiation of Human Pluripotent Stem Cells-Derived Cardiomyocytes and Endothelial Cells from Cardiac Mesoderm Provides a Three-Dimensional Model of Cardiac Microtissue. *Current protocols in human genetics* 2017; **95**: 21.9.1-9.2.
38. Mummery CL, Zhang J, Ng ES, Elliott DA, Elefanty AG, Kamp TJ. Differentiation of human embryonic stem cells and induced pluripotent stem cells to cardiomyocytes: a methods overview. *Circulation research* 2012; **111**(3): 344-58.
39. Zhang J, Klos M, Wilson GF, et al. Extracellular matrix promotes highly efficient cardiac differentiation of human pluripotent stem cells: the matrix sandwich method. *Circulation research* 2012; **111**(9): 1125-36.
40. Sagnella S, Anderson E, Sanabria N, Marchant RE, Kottke-Marchant K. Human endothelial cell interaction with biomimetic surfactant polymers containing Peptide ligands from the heparin binding domain of fibronectin. *Tissue Eng* 2005; **11**(1-2): 226-36.

41. Orlova VV, van den Hil FE, Petrus-Reurer S, Drabsch Y, Ten Dijke P, Mummery CL. Generation, expansion and functional analysis of endothelial cells and pericytes derived from human pluripotent stem cells. *Nature protocols* 2014; **9**(6): 1514-31.
42. Rensen PC, Herijgers N, Netscher MH, Meskers SC, van Eck M, van Berkel TJ. Particle size determines the specificity of apolipoprotein E-containing triglyceride-rich emulsions for the LDL receptor versus hepatic remnant receptor in vivo. *Journal of lipid research* 1997; **38**(6): 1070-84.
43. Rensen PC, van Dijk MC, Havenaar EC, Bijsterbosch MK, Kruijt JK, van Berkel TJ. Selective liver targeting of antivirals by recombinant chylomicrons--a new therapeutic approach to hepatitis B. *Nature medicine* 1995; **1**(3): 221-5.
44. Khedoe PPSJ, Hoeke G, Kooijman S, et al. Brown adipose tissue takes up plasma triglycerides mostly after lipolysis. *Journal of lipid research* 2015; **56**(1): 51-9.
45. Feingold KR, Grunfeld C. Introduction to Lipids and Lipoproteins. In: Feingold KR, Anawalt B, Boyce A, et al., eds. Endotext. South Dartmouth (MA): MDText.com, Inc.; 2000.
46. Berbee JF, van der Hoogt CC, Sundararaman D, Havekes LM, Rensen PC. Severe hypertriglyceridemia in human APOC1 transgenic mice is caused by apoC-I-induced inhibition of LPL. *Journal of lipid research* 2005; **46**(2): 297-306.
47. Giacomelli E, Bellin M, Sala L, et al. Three-dimensional cardiac microtissues composed of cardiomyocytes and endothelial cells co-differentiated from human pluripotent stem cells. *Development (Cambridge, England)* 2017; **144**(6): 1008-17.
48. Ikeda Y, Takagi A, Yamamoto A. Purification and characterization of lipoprotein lipase and hepatic triglyceride lipase from human postheparin plasma: production of monospecific antibody to the individual lipase. *Biochimica et Biophysica Acta (BBA) - Lipids and Lipid Metabolism* 1989; **1003**(3): 254-69.
49. Kuddannaya S, Chuah YJ, Lee MH, Menon NV, Kang Y, Zhang Y. Surface chemical modification of poly(dimethylsiloxane) for the enhanced adhesion and proliferation of mesenchymal stem cells. *ACS applied materials & interfaces* 2013; **5**(19): 9777-84.
50. McCoy MG, Sun GS, Marchadier D, Maugeais C, Glick JM, Rader DJ. Characterization of the lipolytic activity of endothelial lipase. *Journal of lipid research* 2002; **43**(6): 921-9.
51. Yu JE, Han S-Y, Wolfson B, Zhou Q. The role of endothelial lipase in lipid metabolism, inflammation, and cancer. *Histol Histopathol* 2018; **33**(1): 1-10.
52. Bio-Rad. Western Blot Troubleshooting: Unusual or Unexpected Bands. <https://www.bio-rad-antibodies.com/western-blot-unusual-unexpected-bands-western-blotting.html>.
53. NCBI Gene database. Lpl lipoprotein lipase [ Mus musculus (house mouse) ]. <https://www.ncbi.nlm.nih.gov/gene?Db=gene&Cmd=DetailsSearch&Term=16956>
54. Jong MC, Hofker MH, Havekes LM. Role of ApoCs in lipoprotein metabolism: functional differences between ApoC1, ApoC2, and ApoC3. *Arterioscler Thromb Vasc Biol* 1999; **19**(3): 472-84.
55. Kersten S. Physiological regulation of lipoprotein lipase. *Biochimica et biophysica acta* 2014; **1841**(7): 919-33.
56. Olivecrona G, Beisiegel U. Lipid binding of apolipoprotein CII is required for stimulation of lipoprotein lipase activity against apolipoprotein CII-deficient chylomicrons. *Arterioscler Thromb Vasc Biol* 1997; **17**(8): 1545-9.
57. Ranganathan G, Ong JM, Yukht A, et al. Tissue-specific expression of human lipoprotein lipase. Effect of the 3'-untranslated region on translation. *The Journal of biological chemistry* 1995; **270**(13): 7149-55.
58. Febbraio M, Hajjar DP, Silverstein RL. CD36: a class B scavenger receptor involved in angiogenesis, atherosclerosis, inflammation, and lipid metabolism. *The Journal of clinical investigation* 2001; **108**(6): 785-91.
59. Scudellari M. How iPS cells changed the world. *Nature* 2016; **534**(7607): 310-2.
60. Rana P, Anson B, Engle S, Will Y. Characterization of human-induced pluripotent stem cell-derived cardiomyocytes: bioenergetics and utilization in safety screening. *Toxicological sciences : an official journal of the Society of Toxicology* 2012; **130**(1): 117-31.

61. Correia C, Koshkin A, Duarte P, et al. Distinct carbon sources affect structural and functional maturation of cardiomyocytes derived from human pluripotent stem cells. *Scientific Reports* 2017; **7**(1): 8590.
62. Yang X, Pabon L, Murry CE. Engineering adolescence: maturation of human pluripotent stem cell-derived cardiomyocytes. *Circulation research* 2014; **114**(3): 511-23.
63. Mannhardt I, Breckwoldt K, Letuffe-Breniere D, et al. Human Engineered Heart Tissue: Analysis of Contractile Force. *Stem Cell Reports* 2016; **7**(1): 29-42.
64. Lemoine MD, Mannhardt I, Breckwoldt K, et al. Human iPSC-derived cardiomyocytes cultured in 3D engineered heart tissue show physiological upstroke velocity and sodium current density. *Sci Rep* 2017; **7**(1): 5464.
65. Nunes SS, Miklas JW, Liu J, et al. Biowire: a platform for maturation of human pluripotent stem cell-derived cardiomyocytes. *Nature Methods* 2013; **10**: 781.
66. Correia C, Koshkin A, Duarte P, et al. 3D aggregate culture improves metabolic maturation of human pluripotent stem cell derived cardiomyocytes. *Biotechnology and Bioengineering* 2018; **115**(3): 630-44.
67. Ulmer BM, Stoehr A, Schulze ML, et al. Contractile Work Contributes to Maturation of Energy Metabolism in hiPSC-Derived Cardiomyocytes. *Stem Cell Reports* 2018; **10**(3): 834-47.

# Appendix

## Expanded methods

### A.1 Protocol cardiomyocyte seeding (ML-1)

#### Coating of well plate

- Matrigel
  - 31331 medium
  - **12 well plate**
1. Defrost Matrigel on ice and place 31331 medium on ice (otherwise it directly becomes gel when adding the Matrigel)
  2. Prepare Matrigel solution (1:100) by adding **60 µL Matrigel** to **6 mL 31331 medium**
  3. Coat the wells with **0.5 mL/well** of the solution
  4. Incubate 45 min at 37°C

#### Maturation medium for cardiomyocytes (CM-gal-gluc-TI)

- CM-galactose medium
  - T3 (-20°C, store in fridge when open)
  - HCl (fridge)
  - IGF (-80°C, store in fridge when open)
  - Glucose (-20°C, store in fridge when open)
1. Add to **45 mL CM-gal medium**:
    - 150 µL T3**
    - 45 µL HCl**
    - 4.5 µL IGF**
    - 450 µL glucose**

#### Seeding of the cardiomyocytes

- Cardiomyocytes on 6 well plate
  - DPBS
  - TrypLE-select
  - MEF medium
  - CM-gal-gluc-TI medium
1. Aspirate the medium
  2. Wash the cells with **2mL/well DPBS**, gently agitate the wells to make sure the DPBS covers all cells
  3. Aspirate the DPBS directly
  4. Add **1 mL/well TrypLE-Select** (hold the pipette in the middle above the cells, not from against the wall, such that the TrypLE reaches all cells)
  5. Incubate for **10 minutes at 37°C**
  6. Dissociate the cells by pipetting up and down in circles, turn plate around to get cells from all sides (You can use same pipet tip for all wells in same condition)
  7. Transfer cell suspension to 15 mL tube
  8. Add **2 mL/well MEF medium** to the 15 mL tube to stop the trypsinization reaction

9. Add **1 mL/well MEF medium** to rinse remaining cells from the wells, resuspend and add to the 15 mL tube
10. Centrifuge 3 min at 1200 rpm
11. Aspirate MEF medium
12. Add **1 mL CM-gal-gluc-TI medium** to the tube and resuspend very gently!
13. Count cells: **10 µL CMs** and **10 µL Trypan blue**, and add 10 µL to hemacytometer
  - a. Count top right + bottom left square and take average (Leiden: 26 squares)
  - b. Number of cells = average cell count x 2 x 10,000
  - c. Seeding density is 150,000 MCs/well
  - d. Number of wells to seed = number of cells/150,000
14. Aspirate Matrigel from wells plate
15. Cells are already suspended in 1 mL of medium, so add 1 mL/well x number of wells to seed minus 1 mL to the cell suspension
16. Resuspend
17. Seed 1 mL/well
18. Place in incubator and move the well plate 3 times front-to-back and left-to-right (cross shape) over the incubator surface to make sure the cells are evenly spread

## A.2 Protocol endothelial cell seeding and passaging (ML-1)

### Coating of 12 well plate

- Fibronectin
  - DPBS
  - 12 well plate
2. Prepare fibronectin solution (1:200) by adding **30 µL fibronectin** to **6 mL DPBS**
  3. Coat the wells with **0.5 mL/well** of the solution
  4. Incubate at least 1h at 37°C

### Seeding of the endothelial cells on 12 wells plate

- Endothelial cells (LN container: check Excel file "LN storage" in AST folder for stock)
  - BPEL
  - SB
  - VEGF
1. **Prepare medium:** BPEL + SB (1:2000) + VEGF (1:1000)
    - a. Add **12 mL BPEL**, **12 µL VEGF** and **6 µL SB** to a 15mL tube
    - b. Write the date on SB and VEGF tubes, the first time you open a new one (discard after 2 weeks)
  2. Thaw the cells in warm water bad for a few seconds
  3. Add **4 mL BPEL** and **0.5 mL ECs** to a 15 mL tube, then add **1 mL BPEL** to the Eppendorf of the ECs to wash remaining cells out, and add to the 15 mL tube as well
  4. Centrifuge 3 min at 1100 rpm (to wash of freezing medium)
  5. Aspirate BPEL from centrifuged tube
  6. Add 1 mL of prepared medium and resuspend
  7. Count cells: **10 µL ECs** and **10 µL Trypan blue**
    - a. Count 25 hokjes
    - b. Number of cells = cell count x 2 x 10,000
    - c. Seeding density is 100,000 to 150,000 ECs/well

8. Cells are already suspended in 1 mL of medium, so add 1 mL/well x number of wells to seed minus 1 mL to the cell suspension (so if you want to seed 4 wells, add 3 mL)
9. Resuspend
10. **Seed 1 mL/well**
11. Place in incubator and move the plate 3 times front-to-back and left-to-right (cross shape) over the incubator surface to make sure the cells are evenly spread

Passaging the endothelial cells on 12 wells plate

- 1 mL/well BPEL+VEGF+SB medium (see before for preparation)
  - DPBS
  - TrypIE-Select
  - MEF medium
1. Aspirate the medium
  2. Wash the cells with **1 mL/well DPBS**, gently agitate the wells to make sure the DPBS covers all cells
  3. Aspirate the DPBS
  4. Add **0.4 mL/well TrypIE-Select** and incubate the cells for **3 minutes at 37°C**
  5. Dissociate the cells by pipetting up and down
  6. Transfer cell suspension to 50 mL tube
  7. Add **1.5 mL/well MEF medium** to stop the trypsinization reaction
  8. Add **0.5 mL/well MEF medium** to rinse remaining cells from the wells, resuspend and add to the tube
  9. Centrifuge 3 min at 1100 rpm
  10. Remove supernatant, add **1 mL of BPEL+VEGF+SB medium** and resuspend
  11. Count cells: **10 µL ECs** and **10 µL Trypan blue**, and add 10 µL to hemacytometer
    - a. Count 25 hokjes
    - b. Number of cells = cell count x 2 x 10,000
    - c. Seeding density is 100,000 to 150,000 ECs/well
  12. Cells are already suspended in 1 mL of medium, so add 1 mL/well x number of wells to seed minus 1 mL to the cell suspension
  13. Resuspend
  14. **Seed 1 mL/well**
  15. Place in incubator and move the 6 well plate 3 times front-to-back and left-to-right (cross shape) over the incubator surface to make sure the cells are evenly spread

### A.3 Protocol particle experiment (C -lab)

- Particle solution
  - Heparin solution
  - ApoC2 solution
  - DPBS
  - Ultima Gold (*'telvloestof'*)
1. Prepare **heparin solution**
    - a. Dilute Heparin 1:5000 >> for 16 wells: **2 µL Hep / 10 mL DPBS**
  2. [*In case of ApoC2 condition: Prepare ApoC2-solution*]
 

ApoC2 to particle solution should be 1:200 >> 0.25 µL ApoC2 / 50 µL particle solution = 0.05 µL ApoC2 / 10 µL particle solution (= 1 well)

    - a. Dilute ApoC2 1:20 >> For 20 wells: **1 µL ApoC2 / 20 µL medium**

- b. Add **1.05  $\mu\text{L}$ /well ApoC2 solution**
3. Add **10  $\mu\text{L}$ /well particle solution** and incubate the cells for **4 hours at 37°C**
4. Collect the medium and store in Eppendorf tube
5. Wash the cells **2-times** with **0.5 mL/well DPBS** and aspirate directly
6. [*In case of heparin condition: Add **0.5 mL/well heparin solution** and leave for **1 minute** to release/remove the particles between the cells]*
7. Wash the cells with **0.5 mL/well DPBS** and aspirate directly
8. Add **0.3 mL/well DPBS**
9. Scrape the cells from the bottom of the well with a pipet tip, then aspirate the DPBS with the cells and add to a counting tube ('telpotje')
10. Add **2.5 mL/telpotje Ultima Gold**
11. Shake well
12. Place in counting machine (back right), add a flag label, and run program "3h\_14C\_dpm\_5min (endo)" by associating it to the right flag

#### A.4 Medium collection for LPL activity assay (ML-1)

- Heparin 5000U/mL
1. Prepare **heparin solution** (2U/mL)
    - a. Heparin of 5000U/mL >> to get 2U/mL, 0.4  $\mu\text{L}$ /well heparin is needed
    - b. Dilute heparin 1:20 >> For 12 wells: **4.8  $\mu\text{L}$  heparin / 96  $\mu\text{L}$  medium**
    - c. Add **8.4  $\mu\text{L}$ /well heparin solution**
  2. Incubate the cells for **45 minutes at 37°C**
  3. Collect the medium and store in Eppendorf tube in aliquots of 350  $\mu\text{L}$  (or at least 250  $\mu\text{L}$ )
  4. Also, store 1 aliquot of 'clean' medium to test for intrinsic LPL activity

#### A.5 RNA collection (General lab)

- RLT buffer
  - $\beta$ -mercaptoethanol (in hood!)
  - DPBS (or PBS)
1. Collect medium (for LPL assay)
  2. Prepare **RLT +  $\beta$ -mercaptoethanol mix**
    - a. Add together: 10  $\mu\text{L}$   $\beta$ -mercaptoethanol for every 1 mL RLT buffer
    - b. For 16 wells: 5.6 mL RLT buffer + 56  $\mu\text{L}$   $\beta$ -mercaptoethanol
  3. Add **2 mL/well DPBS** to wash and directly aspirate
  4. Add **350  $\mu\text{L}$ /well RLT +  $\beta$ -mercaptoethanol mix**
  5. Dissociate cells by pipetting up and down in circles >> all cells should be lysed
  6. Collect in Eppendorf tube
  7. Store in -20 °C freezer

## A.6 Primer design

1. Search in the NCBI database (<https://www.ncbi.nlm.nih.gov/gene>) for the gene of interest and check the NCBI reference sequence (NM ...). Click on this reference sequence link and click 'pick primers' in the box on the right.
2. Adjust the PCR product size (from min 70 to max 120) and preferably increase the minimum intron length range to minimize the chance on amplifying a genomic DNA product (if the genomic DNA product containing introns is too large, it cannot get amplified)
3. Either change 'exon junction span' to 'primer must span an exon-exon junction', or click the box 'primer pair must be separated by at least one intron on the corresponding genomic DNA'. In the first case the primer anneals on an exon-exon junction which means the primer cannot anneal to genomic DNA containing introns, and in the second case the forward primer anneals to one exon, and the reverse primer to another. Both methods have their advantages and disadvantages.
4. Click on get primers, and inspect the region of the gene which will be amplified by the primers.
5. Go to Ensembl (<https://www.ensembl.org/index.html>) and search for the gene of interest. Inspect the protein-coding regions of the gene (the ones that have a RefSeq are the best characterized), and select a primer in the NCBI results that amplifies the region that contains (most of) these protein-coding regions of the gene.
6. Run an in silico PCR to check the PCR products by going to the UCSC Genome Bioinformatics website (<https://genome.ucsc.edu/>) and select 'In Silico PCR' under 'Tools'. Under 'Target', either select genome assembly or UCSC genes. With genome assembly you can check whether the primers amplify a genomic DNA product (does not matter when the product is > 1000 kb). With UCSC genes you can check whether the PCR amplifies your mRNA of interest.
7. Always run an in silico PCR with primer sequences obtained from literature.

## Supplementary tables

**Supplementary Table 1.** CT values for *CD36*, *LPL*, *GPIHBP1*, *LIPG* and the housekeeping gene *RPL37A* as determined by qRT-PCR.

Sample no.	Group	Gene	CT duplicate 1	CT duplicate 2	Mean CT
1	Cardiomyocytes	<i>LPL</i>	26.85	26.42	26.64
2	Cardiomyocytes	<i>LPL</i>	26.82	28.66	27.74
3	Cardiomyocytes	<i>LPL</i>	27.83	27.64	27.74
4	Cardiomyocytes	<i>LPL</i>	27.13	27.1	27.12
5	Co-culture	<i>LPL</i>	25.83	25.95	25.89
6	Co-culture	<i>LPL</i>	26.55	27.32	26.94
7	Co-culture	<i>LPL</i>	26.26	26.5	26.38
8	Co-culture	<i>LPL</i>	27.18	27.38	27.28
9	Endothelial cells	<i>LPL</i>	27.2	26.85	27.03
10	Endothelial cells	<i>LPL</i>	28.54	28.47	28.51
11	Endothelial cells	<i>LPL</i>	27.6	27.49	27.55
12	Endothelial cells	<i>LPL</i>	27.06	27.08	27.07
minRT1	Cardiomyocytes	<i>LPL</i>	N/A	N/A	N/A
minRT5	Co-culture	<i>LPL</i>	38.64	N/A	N/A
minRT9	Endothelial cells	<i>LPL</i>	35.58	39.22	37.40
H2O		<i>LPL</i>	N/A	39.69	N/A
1	Cardiomyocytes	<i>CD36</i>	26.40	26.35	26.38
2	Cardiomyocytes	<i>CD36</i>	27.04	26.65	26.85
3	Cardiomyocytes	<i>CD36</i>	26.85	26.95	26.90
4	Cardiomyocytes	<i>CD36</i>	27.17	26.48	26.83
5	Co-culture	<i>CD36</i>	25.49	26.16	25.83
6	Co-culture	<i>CD36</i>	25.60	26.02	25.81
7	Co-culture	<i>CD36</i>	26.20	26.4	26.30
8	Co-culture	<i>CD36</i>	27.52	27.58	27.55
9	Endothelial cells	<i>CD36</i>	30.36	30.68	30.52
10	Endothelial cells	<i>CD36</i>	31.08	31	31.04
11	Endothelial cells	<i>CD36</i>	30.78	30.79	30.79
12	Endothelial cells	<i>CD36</i>	30.07	30.3	30.19
minRT1	Cardiomyocytes	<i>CD36</i>	N/A	N/A	N/A
minRT5	Co-culture	<i>CD36</i>	N/A	N/A	N/A
minRT9	Endothelial cells	<i>CD36</i>	N/A	N/A	N/A
H2O		<i>CD36</i>	N/A	N/A	N/A
1	Cardiomyocytes	<i>GPIHBP1</i>	N/A	N/A	N/A
2	Cardiomyocytes	<i>GPIHBP1</i>	N/A	39.36	N/A
3	Cardiomyocytes	<i>GPIHBP1</i>	N/A	N/A	N/A
4	Cardiomyocytes	<i>GPIHBP1</i>	N/A	N/A	N/A
5	Co-culture	<i>GPIHBP1</i>	N/A	N/A	N/A
6	Co-culture	<i>GPIHBP1</i>	N/A	N/A	N/A
7	Co-culture	<i>GPIHBP1</i>	N/A	N/A	N/A
8	Co-culture	<i>GPIHBP1</i>	N/A	N/A	N/A
9	Endothelial cells	<i>GPIHBP1</i>	26.62	26.76	26.69
10	Endothelial cells	<i>GPIHBP1</i>	28.48	28.27	28.38

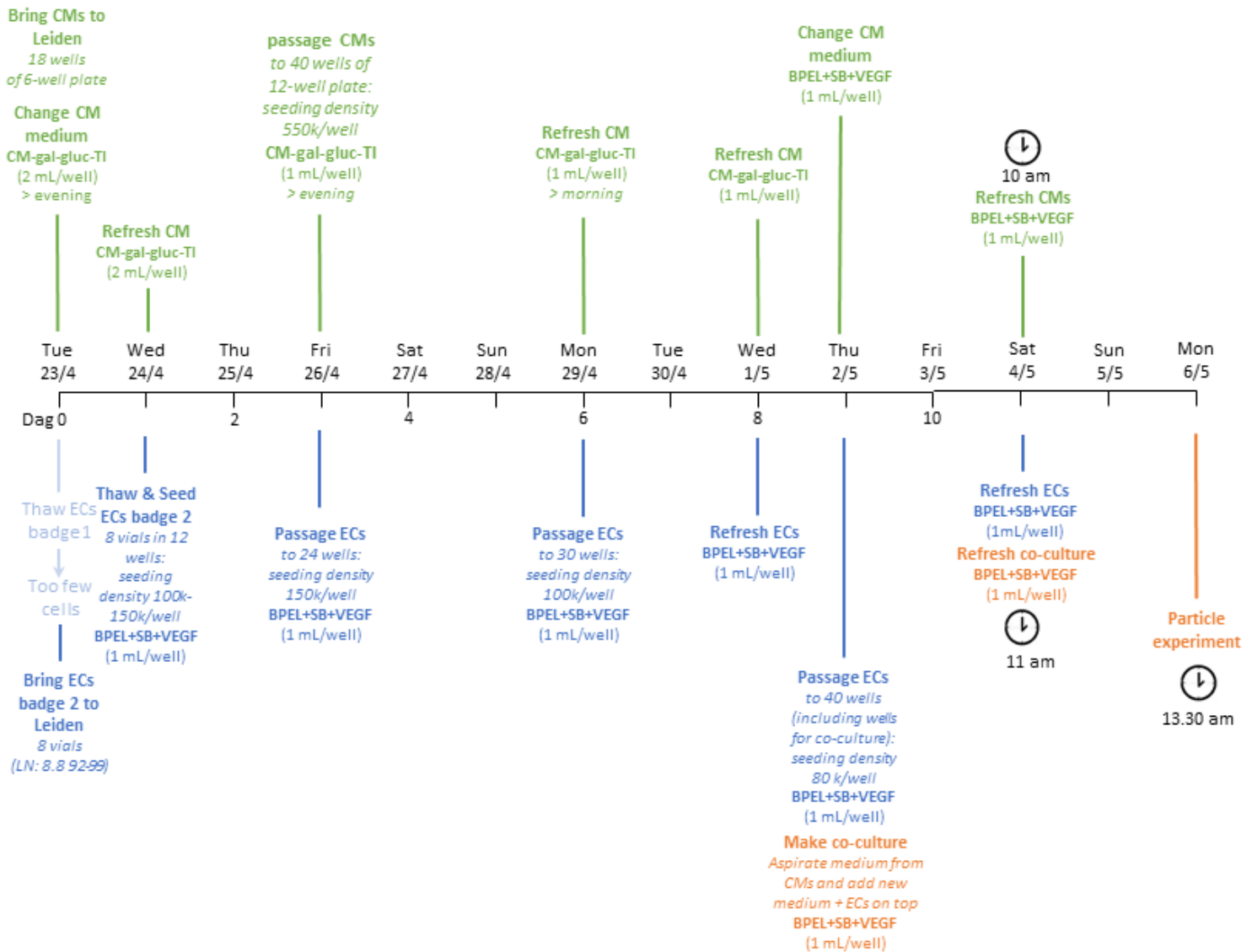
11	Endothelial cells	<i>GPIHBP1</i>	30.85	30.27	30.56
12	Endothelial cells	<i>GPIHBP1</i>	32	32.45	32.23
minRT1	Cardiomyocytes	<i>GPIHBP1</i>	27.75	28.37	28.06
minRT5	Co-culture	<i>GPIHBP1</i>	26.34	26.28	26.31
minRT9	Endothelial cells	<i>GPIHBP1</i>	28.12	27.93	28.03
H2O		<i>GPIHBP1</i>	30.32	30.19	30.26
1	Cardiomyocytes	<i>LIPG</i>	N/A	N/A	N/A
2	Cardiomyocytes	<i>LIPG</i>	N/A	N/A	N/A
3	Cardiomyocytes	<i>LIPG</i>	N/A	N/A	N/A
4	Cardiomyocytes	<i>LIPG</i>	N/A	N/A	N/A
5	Co-culture	<i>LIPG</i>	N/A	N/A	N/A
6	Co-culture	<i>LIPG</i>	N/A	N/A	N/A
7	Co-culture	<i>LIPG</i>	N/A	N/A	N/A
8	Co-culture	<i>LIPG</i>	N/A	N/A	N/A
9	Endothelial cells	<i>LIPG</i>	N/A	N/A	N/A
10	Endothelial cells	<i>LIPG</i>	N/A	N/A	N/A
11	Endothelial cells	<i>LIPG</i>	N/A	N/A	N/A
12	Endothelial cells	<i>LIPG</i>	N/A	N/A	N/A
minRT1	Cardiomyocytes	<i>LIPG</i>	N/A	N/A	N/A
minRT5	Co-culture	<i>LIPG</i>	N/A	N/A	N/A
minRT9	Endothelial cells	<i>LIPG</i>	N/A	N/A	N/A
H2O		<i>LIPG</i>	N/A	N/A	N/A

## Supplementary figures

### Co-culture experiment 3 | April 2019

For particle experiment time series

Performed on 12 wells plate: total 60 wells



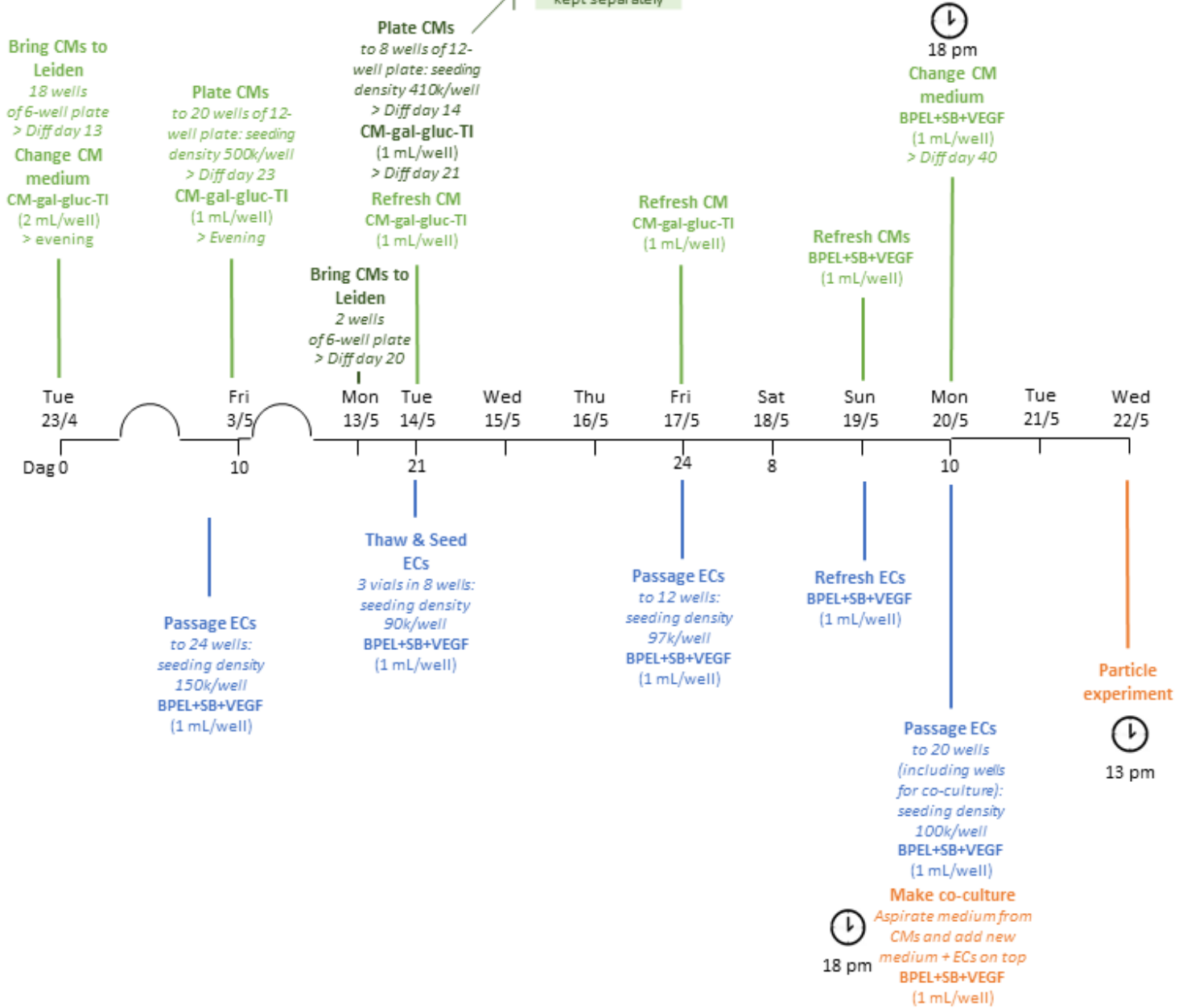
**Supplementary figure 1.** Experiment planning “Effects of particle incubation time on fatty acid uptake”. BPEL+SB+VEGF, medium for endothelial cells and co-cultures (see Methods for explanation), CM, cardiomyocytes; CM-gal-gluc-TI, medium for cardiomyocytes (see Methods for explanation); EC, endothelial cells.

**Co-culture experiment 4 | May 2019**

For ApoC2 concentrations

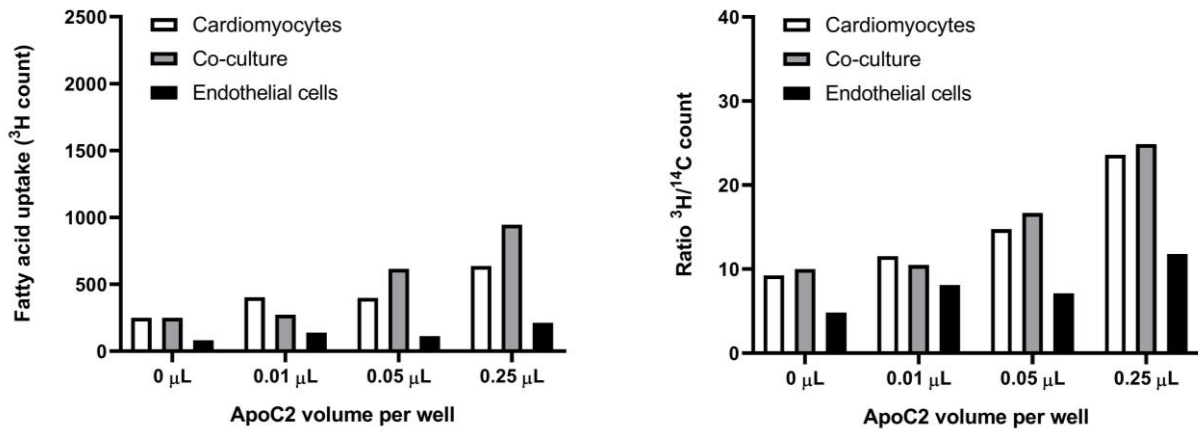
Performed on 12 wells plate: total 38 wells

8 new wells used for same experiment, but kept separately

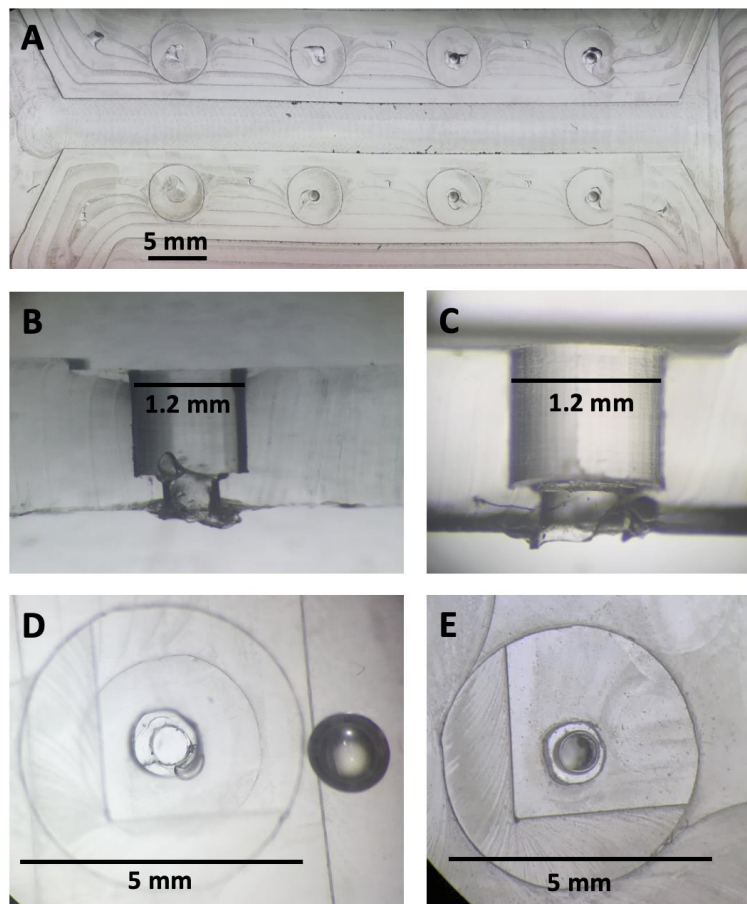


**Supplementary figure 2.** Experiment planning “Dependency of fatty acid uptake on ApoC2”. BPEL+SB+VEGF, medium for endothelial cells and co-cultures (see Methods for explanation), CM, cardiomyocytes; CM-gal-gluc-TI, medium for cardiomyocytes (see Methods for explanation); EC, endothelial cells.





**Supplementary figure 4. Fatty acid uptake by the cells.** Cells were incubated with tri[ $^3\text{H}$ ]oleate and [ $^{14}\text{C}$ ]cholesteryl oleate double labeled TRL-like particles. These particles were pre-incubated with different concentrations of ApoC2, i.e. 0  $\mu\text{L}/\text{well}$ , 0.01  $\mu\text{L}/\text{well}$ , 0.05  $\mu\text{L}/\text{well}$  or 0.25  $\mu\text{L}/\text{well}$ . **(A)** Cellular uptake of fatty acids ( $^3\text{H}$  count) and **(B)** uptake ratio of  $^3\text{H}$  versus  $^{14}\text{C}$  in cardiomyocytes, co-cultures and endothelial cells. Values represent mean  $\pm$  SEM. N is number of wells: N=1 per concentration per cell culture group. ApoC2, apolipoprotein C2.



**Supplementary figure 5. Flaws in non-optimized chip designs.** **(A)** Chipping of the mold resulting in irregularities. **(B, C)** Cross sections of PDMS chip showing irregularities in the PDMS, resulting in blockage of the cell culture spaces. **(D)** Top view of the PDMS chip showing air bubbles in the PDMS. **(E)** Top view of the top mold, showing non-circular shapes of the cylinders.

# Glossary

<b>Acetyl coenzyme A (Acetyl-CoA):</b>	Key enzyme in cellular energy production that is oxidized to produce energy.
<b>Adenosine triphosphate (ATP):</b>	Molecule that is used to store energy in cells. Upon conversion to adenosine diphosphate (ADP) the stored energy is released to drive biological processes.
<b>Angiopietin-like 3 (Angptl3):</b>	Protein that inhibits the LPL.
<b>Apolipoprotein (Apo):</b>	Structural protein components of lipoproteins that are grouped in different classes and have a variety of functions in lipoprotein metabolism, including synthesis, catabolism and uptake.
<b>Apolipoprotein C2 (ApoC2):</b>	Apolipoprotein that is an essential co-factor for LPL enzymatic activity.
<b>(3-aminopropyl)triethoxy silane (APTES):</b>	Aminosilane that can be used for the chemical functionalization of PDMS to enhance the binding of biological molecules.
<b>Bovine serum albumin (BSA) polyvinylalcohol essentials lipids (BPEL) medium:</b>	Medium that was used for culturing endothelial cells and cardiomyocyte-endothelial cell co-cultures.
<b>β2-microglobulin (Beta2):</b>	Gene that encodes for a component of MHC class I molecules. It is expressed in most cells of the body, and therefore frequently used as housekeeping gene for qRT-PCR.
<b>Cardiomyocytes (CM):</b>	Contractile cells of the heart.
<b>Cholesterol (C):</b>	Organic molecule that is a structural component of all human cell membranes, as well as several hormones. It is transported through the blood stream in lipoprotein particles.
<b>Cluster of differentiation 36 (CD36):</b>	Cell membrane protein that transports free fatty acids into the cells.
<b>Co-cultures (Co):</b>	Cell culture consisting out of two or more different cell types. In this study co-cultures refer to co-cultures of cardiomyocytes and endothelial cells.

<b>Cycle quantification value (CT):</b>	Number of polymerase chain reaction cycles that is required to detect a single from the samples using the qRT-PCR technique.
<b>Dulbecco's phosphate buffered saline (DPBS):</b>	Water-based salt solution with a similar pH as the human that is frequently used in biological research to wash cells.
<b>Endothelial cells (EC):</b>	Cells that line the inner surfaces of blood vessels.
<b>Endothelial lipase (LIPG):</b>	Enzyme secreted by endothelial cells that catalyzes the hydrolysis of lipids. It has a similar function as the enzyme LPL.
<b>Glycosylphosphatidylinositol anchored high density lipoprotein binding protein 1 (GPIHBP1):</b>	Protein that is expressed by endothelial cells to bind LPL in the interstitial space and transports in to the luminal side of endothelial cells, where LPL can bind circulating triglyceride rich lipoproteins (TRL).
<b>Heparin (Hep):</b>	Molecule that is mainly known for its pharmaceutical effect: inhibition of blood coagulation. In experimental research it can also be used to free LPL from cell surfaces.
<b>Human induced pluripotent stem cells (hiPSC):</b>	Human pluripotent stem cells (hPSC) that are made by reprogramming skin or urine cells from any individual back into the stem cell state, from which they can be differentiated into any cell type of the human body.
<b>Human pluripotent stem cells (hPSC):</b>	Stem cells that are derived from human embryonic or somatic adult cells. These cells have the capacity to be expanded <i>in vitro</i> and differentiated to any cell type of the human body.
<b>Hydrochloric acid (HCl):</b>	Medium component that was added to the cardiomyocyte medium to keep pH levels optimal for the cells.
<b>Insulin like-growth factor (IGF):</b>	Growth factor that was added to the cardiomyocyte medium.
<b>LDL receptor related protein 10 (LRP10):</b>	Gene that can be used as housekeeping gene for cardiomyocyte-endothelial cell co-cultures in qRT-PCR.
<b>Lipoprotein lipase (LPL):</b>	Key enzyme in energy metabolism by supplying metabolically active tissue with fuel in the form of free fatty acids. LPL activation is a novel pharmaceutical target to reduce cardiovascular disease.

<b>Low-density lipoprotein (LDL):</b>	Medium-sized lipoprotein that transports lipids through the blood stream, having a low ratio of proteins to lipids (hence its name 'low density'), and mainly carrying cholesterol esters in its core. High LDL-cholesterol levels are a risk factor for atherosclerosis formation and consequently cardiovascular disease.
<b>Messenger RNA (mRNA):</b>	Transcript of DNA that transports genetic information to the ribosomes, where it is converted into proteins.
<b>Polydimethylsiloxane (PDMS):</b>	Polymer that is commonly used for soft lithography due to its flexible nature. PDMS is suitable for cell culturing.
<b>Poly(methyl methacrylate) (PMMA):</b>	Polymer, better known as 'Plexiglass'. In this study PMMA was used to fabricate the molds for making the PDMS chip.
<b>Proprotein convertase subtilisin/kexin type 9 (PCSK9):</b>	Enzyme that enhances the break-down of LDL-receptors in the liver. PCSK9 inhibitors have been developed to reduce circulating LDL-cholesterol levels by preventing the break-down of LDL-receptors in the liver, such that more LDL are available to remove LDL particles from the bloodstream.
<b>Ribosomal protein lateral stalk subunit P0 (RPLP0):</b>	Gene that can be used as housekeeping gene for cardiomyocyte-endothelial cell co-cultures in qRT-PCR.
<b>Ribosomal protein L37a (RPL37A):</b>	Gene that can be used as housekeeping gene for cardiomyocyte-endothelial cell co-cultures in qRT-PCR.
<b>RNA purification and quantitative real-time polymerase chain reaction (qRT-PCR):</b>	Method to quantify the gene expression (mRNA) in biological samples.
<b>Standard error of the mean (SEM):</b>	Statistic measure of the variance of the sampling distribution.
<b>Transforming growth factor-<math>\beta</math> pathway small-molecule inhibitor SB431542 (SB):</b>	Medium component that was added to the endothelial cell medium to prevent the transformation of cells into fibroblasts.
<b>Triglyceride (TG):</b>	Esters composed of glycerol and three fatty acids. Triglycerides are the main storage form of fat in the body.
<b>Triglyceride-rich lipoprotein (TRL):</b>	Lipoproteins with a relative high amount of triglycerides in their core compared to the amount of cholesteryl esters. TRLs include VLDL particles and chylomicrons.
<b>Triiodothyronine (T3):</b>	Growth factor that was added to the cardiomyocyte medium.

**Vascular endothelial growth factor (VEGF):**

Growth factor that was added to the endothelial cell medium.

**Very low-density lipoprotein (VLDL):** Large-sized lipoprotein that transports lipids from the liver via the blood stream to peripheral tissue. VLDL particles have a very low ratio of proteins to lipids (hence its name 'very low density'), and mainly carry triglycerides in their core.

**<sup>14</sup>C:** Radio-labelled carbon atom in cholesteryl oleate, which is a cholesteryl ester that is used to form triglyceride-rich lipoprotein-like particles in the lab.

**<sup>3</sup>H:** Radio-labelled hydrogen atom in trioleate, which is a triglyceride that is used to form triglyceride-rich lipoprotein-like particles in the lab.